

University of Nebraska - Lincoln

DigitalCommons@University of Nebraska - Lincoln

Theses, Dissertations, and Student Research from
Electrical & Computer Engineering

Electrical & Computer Engineering, Department of

11-2014

UV LASER-ASSISTED DIAMOND DEPOSITION

Mengxiao Wang

University of Nebraska - Lincoln, chlywmx@gmail.com

Follow this and additional works at: <http://digitalcommons.unl.edu/elecengtheses>



Part of the [Electrical and Electronics Commons](#), and the [Engineering Science and Materials Commons](#)

Wang, Mengxiao, "UV LASER-ASSISTED DIAMOND DEPOSITION" (2014). *Theses, Dissertations, and Student Research from Electrical & Computer Engineering*. 60.

<http://digitalcommons.unl.edu/elecengtheses/60>

This Article is brought to you for free and open access by the Electrical & Computer Engineering, Department of at DigitalCommons@University of Nebraska - Lincoln. It has been accepted for inclusion in Theses, Dissertations, and Student Research from Electrical & Computer Engineering by an authorized administrator of DigitalCommons@University of Nebraska - Lincoln.

UV LASER-ASSISTED DIAMOND DEPOSITION

by

Mengxiao Wang

A THESIS

Presented to the Faculty of

The Graduate College at the University of Nebraska

In Partial Fulfillment of Requirements

For the Degree of Master of Science

Major: Electrical Engineering

Under the Supervision of Professor Yongfeng Lu

Lincoln, Nebraska

Nov, 2014

UV LASER-ASSISTED DIAMOND DEPOSITION

Mengxiao Wang, M.S.

University of Nebraska, 2014

Adviser: Yongfeng Lu

Diamond, due to its unique properties, has been studied for decades. Many diamond synthesis methods have been developed as well. As one of the synthesis methods, combustion flame chemical vapor deposition (CVD) is considered as the most flexible way. Combined with laser irradiation, laser-assisted combustion flame CVD can enhance the deposition process of diamond films. In this thesis work, efforts were made to explore the capability of a laser-assisted combustion flame CVD technique with krypton fluoride (KrF) excimer laser irradiation for improving diamond thin film quality and deposition rate. The research efforts mainly focus on following activities, including: 1) studying the influence of the gap distance between the inner flame and the substrates on crystallographic orientations, quality and deposition rate of the diamond film to determine the optimal parameters for the deposition; 2) conducting *in-situ* KrF excimer laser irradiation during the deposition process to increase the quality and the growth rate of the diamond film with the optimal deposition parameters, which includes excimer laser irradiation on the diamond film and on the combustion flame; 3) applying *post-growth* KrF excimer laser irradiation on diamond films, which is aiming to understand and verify the effect of KrF excimer laser irradiation on the diamond film during the deposition. A

multi-torch combustion flame CVD was also developed for increasing the efficiency of depositing large-area diamond thin films.

Diamond thin films have been deposited on tungsten carbide (WC) by the laser-assisted combustion-flame CVD technique in open atmosphere. A KrF excimer laser was used in the process to: 1) achieve energy coupling into combustion flame; 2) influence species proportions in the combustion flame; 3) promote seeding and nucleation process during diamond film deposition; 4) increase the diamond thin film quality and deposition rate through non-diamond carbon removal. Observations from experimental results confirmed that excimer laser irradiation could promote seeding and nucleation of diamond, growth rate and diamond quality. Furthermore, by changing the gap distance, the crystallographic orientations of diamond films can be controlled successfully and the optimal gap distance for diamond deposition can also be found. With applying a multi-torch setup in laser-assisted combustion flame CVD method, large-area diamond thin films were synthesized efficiently.

ACKNOWLEDGEMENTS

With the two-and-half-year study, I will finish my Master degree at the University of Nebraska – Lincoln. Throughout this period of time, I received much help from many nice and friendly people who will be my mentors and friends in my whole life. I would like to express my sincere gratitude to those people who gave me instruction and advices for my study and life. First of all, I would like to thank my advisor, Professor Yongfeng Lu, who gave me his generous support to not only my study but also my life. Professor Lu has shared his wisdom and life experience with me. Self-motivation, responsibility, confidence, diligence and meticulousness are the most valuable qualities that I learned from Professor Lu.

Secondly, I would like to deliver my special thanks to Professor Natale J. Ianno from the Department of Electrical Engineering at UNL and Professor Xiao Cheng Zeng from the Department of Chemistry at UNL for serving on my master supervisory committee.

Then, I would like to thank Dr. Yunzhen Zhou and Ms. Lisha Fan from the Department of Electrical Engineering at UNL. Their theoretical support has helped me very much in my research work.

I also would like to deliver many thanks to Professors Dennis R. Alexander and Mathias Schubert from the Department of Electrical Engineering at UNL for providing their help to get access to their labs and equipment such as stylus profiler and scanning electron microscopy (SEM). Many thanks are given to Dr. Craig Zuhlke in Professor

Dennis R. Alexander's group for helping me operate SEM as well. I am grateful to Drs. Han Chen and You Zhou from the Center for Biotechnology Core Research Facilities (CBCRF) at UNL for their help on SEM.

I really thank all my friends and colleagues: Drs. Xiangnan He, Yang Gao, Wei Xiong, Dawei Li, Jinzhong Lu, Huifu Luo, Jin Sun, Wei Qiu, Shizhen Xu, Thomas Guillemet, Premkumar Thirugnanam and Masoud Mahjouri-Samani; Misters Lijia Jiang, Xi Huang, Mengmeng Wang, Hossin Rabiei, Yao Lu, Chenfei Zhang, Kamran Keramatnejad, Ufuk Kilic and Qiming Zou; Ms. Lei Liu; Misses Wenjia Hou, Ying Liu and Clio Azina, and many other friends. I appreciate their generous help and support on my research work and life.

Finally, I feel greatly indebted to my family, particularly my parents, Mr. Wei Wang and Ms. Cuifeng Wang, and my Uncle, Mr. Jiandong Wang. They have been supporting and will support me without any reservation in all respects of my life. Without their support, it would have been very hard for me to get through the Master studies.

TABLE OF CONSTANTS

ACKNOWLEDGEMENTS	I
TABLE OF CONSTANTS	III
LIST OF FIGURES	V
LIST OF TABLES	IX
CHAPTER 1 Introduction	1
1.1 Introduction to laser-assisted material synthesis	2
1.2 Introduction to diamond	4
1.2.1 <i>General properties of diamond</i>	4
1.2.2 <i>Diamond deposition</i>	4
1.3 Motivation	8
1.4 Thesis outline	11
CHAPTER 2 Growth of Diamond Films with Different Gap Distance	19
2.1 Introduction	20
2.2 Experiments, results and discussion	22
2.2.1 <i>Growth of diamond films</i>	22
2.2.2 <i>Characterization of diamond films</i>	25
2.3 Conclusions	30

CHAPTER 3	<i>In-situ</i> Excimer Laser Irradiation during Diamond Film Deposition	34
3.1	Introduction	35
3.2	Experiments, results and discussion	38
3.2.1	<i>Excimer laser irradiation on the diamond film</i>	38
3.2.2	<i>Excimer laser irradiation on the flame</i>	45
3.2.3	<i>Post-growth excimer laser irradiation on diamond films</i>	59
3.3	Conclusions	64
CHAPTER 4	Multi-torch Diamond Film Deposition	69
4.1	Introduction	70
4.2	Experiments, results and discussion	71
4.3	Conclusions	77
CHAPTER 5	Summary of Current Work and Suggested Future Directions	81
5.1	Summary of current work	82
5.2	Suggested future directions	85
LIST OF PUBLICATIONS		87

LIST OF FIGURES

Figure 1.1 The carbon phase diagram [35] showing that diamond is a high-temperature-high-pressure carbon phase.	5
Figure 2.1 A schematic diagram of combustion flame CVD.	23
Figure 2.2 A typical optical image of the C ₂ H ₄ /C ₂ H ₂ /O ₂ combustion flame.	23
Figure 2.3 A schematic diagram showing the gap distance between the inner flame and the substrate.	24
Figure 2.4 Typical SEM images of diamond films with gap distance of (a) 0.2, (b) 0.3, (c) 0.4, (d) 0.5, (e) 0.6, (f) 0.7 and (g) 0.8 mm gap distance, respectively.	26
Figure 2.5 (a) Thickness of diamond films deposited with different gap distance and (b) the relationship between gap distance and film thickness.	27
Figure 2.6 (a) Typical Raman spectra of diamond films deposited with different gap distance and (b) the relationship between gap distance and diamond quality factor.	29
Figure 3.1 A schematic diagram showing electron excitation of carbon atoms.	36
Figure 3.2 A schematic diagram showing the experimental setup for diamond films deposited using KrF excimer laser irradiation on the diamond film.	39
Figure 3.3 Typical SEM images of diamond films deposited (a) without excimer laser, with excimer laser irradiation at fluences of (b) 52.8, (c) 63.3, (d) 70.5, (e) 77.8 and (f) 85 mJ/cm ² , respectively.	40

Figure 3.4 (a) Thickness of diamond films deposited with excimer laser irradiation at different laser fluences on the diamond films and (b) the relationship between laser fluence and film thickness.	42
Figure 3.5 (a) Typical Raman spectra of diamond films deposited with excimer laser irradiation at different laser fluences on the diamond films and (b) the relationship between laser fluence and diamond quality factor.	43
Figure 3.6 A schematic diagram showing the experimental setup for diamond film deposition with KrF excimer laser irradiation on the combustion flame.	45
Figure 3.7 Typical SEM images of diamond films deposited (a) without excimer laser irradiation on the flame, and with excimer laser irradiation at fluences of (b) 105.5, (c) 126.5, (d) 141, (e) 155.5, (f) 170, (g) 185, (h) 199.5, (i) 214 and (j) 229 mJ/cm ² , respectively.	47
Figure 3.8 (a) Thickness of diamond films deposited with excimer laser irradiation at different laser fluences on the flame and (b) the relationship between laser fluence and film thickness.	49
Figure 3.9 (a) Typical Raman spectra of diamond films deposited with excimer laser irradiation at different laser fluences on the flame and (b) the relationship between laser fluence and diamond quality factor.	50
Figure 3.10 Typical SEM images of diamond films deposited (a) without excimer laser irradiation on the flame, and with excimer laser irradiation at frequencies of (b) 1, (c) 5, (d) 10, (e) 15, (f) 20, (g) 25, (h) 30 and (i) 35 Hz, respectively.	52
Figure 3.11 (a) Thickness of diamond films deposited with excimer laser irradiation at different laser frequencies on the flame and (b) the relationship between laser frequency and film thickness.	54

Figure 3.12 (a) Typical Raman spectra of diamond films deposited with excimer laser irradiation at different laser frequencies on the flame and (b) the relationship between laser frequency and diamond quality factor.	55
Figure 3.13 Absorption of excimer laser (a) at different frequencies from 1 to 35 Hz and (b) at different fluence from 105.5 to 229 mJ/cm ² by C ₂ H ₄ /C ₂ H ₂ /O ₂ combustion flame.	57
Figure 3.14 A schematic diagram showing the experimental setup for <i>post-growth</i> KrF excimer laser irradiation on diamond films.	59
Figure 3.15 Typical SEM images of a diamond film (a) not irradiated by excimer laser, irradiated by excimer laser with (b) 10, (c) 20, (d) 30, (e) 40 and (f) 50 pulses, respectively.	60
Figure 3.16 (a) Typical Raman spectra of the sample diamond film not irradiated by excimer laser, irradiated by excimer laser with 10, 20, 30, 40 and 50 pulses and (b) the relationship between the number of laser pulses and diamond quality factor.	62
Figure 4.1 A schematic diagram of the experimental setup for large continuous diamond thin films deposition using combustion flame CVD with CO ₂ laser excitation.	71
Figure 4.2 Images of multi-torch flames (a) without laser, (b) with CO ₂ laser resonant vibrational excitation at 10.532 μm, 800 W.	72
Figure 4.3 An optical image of diamond thin film.	73
Figure 4.4 Typical SEM images of diamond thin films deposited with 10.532 μm CO ₂ laser excitation at different deposition time per step of (a) 15, (b) 10 and (c) 5 min and (d) without CO ₂ laser excitation at a deposition time per step of 10 min, respectively.	73

Figure 4.5 Thickness of diamond films deposited with 10.532 μm CO_2 laser excitation at different deposition time per step of 15, 10 and 5 min and without CO_2 laser excitation at a deposition time per step of 10 min.	75
Figure 4.6 Raman spectra of diamond films deposited with 10.532 μm CO_2 laser excitation at different deposition time per step of 15, 10 and 5 min and without CO_2 laser excitation at a deposition time per step of 10 min.	76
Figure 5.1 Optical emission spectra of $\text{C}_2\text{H}_4/\text{C}_2\text{H}_2/\text{O}_2$ combustion flame.	86

LIST OF TABLES

Table 1.1 Materials deposited by LCVD.	2
---	---

CHAPTER 1

Introduction

1.1 Introduction to laser-assisted material synthesis

1.2 Introduction to diamond

1.2.1 General properties of diamond

1.2.2 Diamond deposition

1.3 Motivation

1.4 Thesis outline

1.1 Introduction to laser-assisted material synthesis

Laser material processing has become an expanding field and been well-established in a wide variety of industrial applications [1-4]. In mechanical area, laser welding, soldering, drilling and cutting were included [1,2]. In metals technology, laser hardening, rapid solidification, glazing, cladding and powder metallurgy have been studied [1,2]. Laser recrystallization, doping and annealing were applied in semiconductor area [3,4]. Laser chemical processing plays an important role in efficiently assisting thin film deposition [5]. Laser-assisted chemical vapor deposition (LCVD) is also widely used to synthesize a variety of materials, such as metals (from metal halides, alkyls, and carbonyls), semiconductors (like amorphous and crystalline germanium, silicon, and compound semiconductors), insulators (like oxides and nitrides), and heterostructures [5]. Table 1.1 lists some typical materials deposited by LCVD processes with specific lasers and wavelengths, and gas precursors.

Table 1.1 Materials deposited by LCVD.

Materials	Gas	Substrates	Laser [wavelength (nm)]	References
Diamond	CH ₄ /H ₂	Si	CO ₂ (10.6 μm)	[6]
Diamond-like carbon	C ₆ H ₆	W	KrF (248)	[7]
SiO ₂	SiH ₄ /N ₂ O	Si	Tunable CO ₂ (10.6, 10.28, 9.6, 9.28 μm)	[8]
W	WF ₆ /SiH ₂	GaAs	KrF (248)	[9,10]
a-CN _x (x<1.3)	C ₂ H ₂ /N ₂ O/ NH ₃	SiO ₂ , Al ₂ O ₃ , Ti/Al ₂ O ₃	CO ₂ (10.6 μm), KrF (248), ArF (193)	[11]

LCVD opens up new possibilities in materials synthesis by enabling new reaction pathways and altered kinetics. In particular, at parallel incidence to the substrate surface, lasers permit pure gas-phase excitation without substrate heating. This is one of the main advantages of LCVD. Intense efforts have been made in the LCVD of high-quality thin films at low substrate temperatures [5]. Successful LCVD of compound semiconductor films at low substrate temperatures have been reported, including gallium arsenide [12], gallium phosphide [13], indium phosphide [14], cadmium telluride [15], and mercury telluride [16]. With low substrate temperatures, interdiffusion of elements at interfaces between films as well as thermal defects were significantly suppressed.

Laser irradiation can induce chemical reactions either homogeneously within the gas or liquid phase or heterogeneously at gas-solid [17] and liquid-solid [18,19] interfaces. In general, laser chemical processing involves photothermal and photochemical processes. In a photothermal process, multiple photons in visible infrared (Vis-IR) range are absorbed to elevate molecules to higher vibrational levels until an atom is ionized or a molecule is dissociated [17]. In a photochemical process, by absorption of visible ultraviolet (UV-Vis) photons, molecules can be electronically dissociated in a single step [18].

Previously, as an approach of LCVD, laser-induced multi-energy processing (MEP) was developed in Laser Assisted Nano Engineering Lab (LANE) [20,21] to increase efficiency of energy coupling, promote growth rate and quality of materials, and control the chemical reaction in CVD process.

1.2 Introduction to diamond

1.2.1 General properties of diamond

As a form of carbon, diamond has been known for a long time. Natural diamond is used all over the world but its storage is extremely rare comparing with graphite and amorphous carbon. Due to its isometric-hexoctahedral crystal structure, diamond is known as the hardest mineral with high dispersion of light. Therefore, diamond is widely used for industrial application and jewelry. Other properties of diamond is also appealing, including high thermal conductivity, high electrical resistivity, low coefficient of friction, high chemical inertness, large band-gap, high breakdown voltage, high carrier mobility and high workable temperature [22]. These attractive properties of diamond make it used as functional coating for surface protection [23], optical window [24], thermal management [25], wear resistance [26], active electronic devices [27], sensors [28], acoustic speakers [29] and photon [30] and electron emitters [31].

1.2.2 Diamond deposition

Since the first diamond synthesis was achieved in 1955 [32], diamond deposition with different strategies has been developed [32-34], which can be divided into high-pressure deposition and low-pressure deposition. Fig. 1.1 shows the carbon phase diagram [35]. According to that phase diagram, diamond is a high-temperature-high-pressure carbon phase consisting of sp^3 hybridized carbon atoms. Therefore, under a high pressure, diamond synthesis can be successfully achieved [36], such as high pressure, high temperature (HPHT) method. Under low pressure, diamond synthesis is achieved from different concepts, such as chemical vapor deposition (CVD) which realizes

diamond growth by adding carbon atoms at a time to the initial substrate to form diamond bond [37-39].

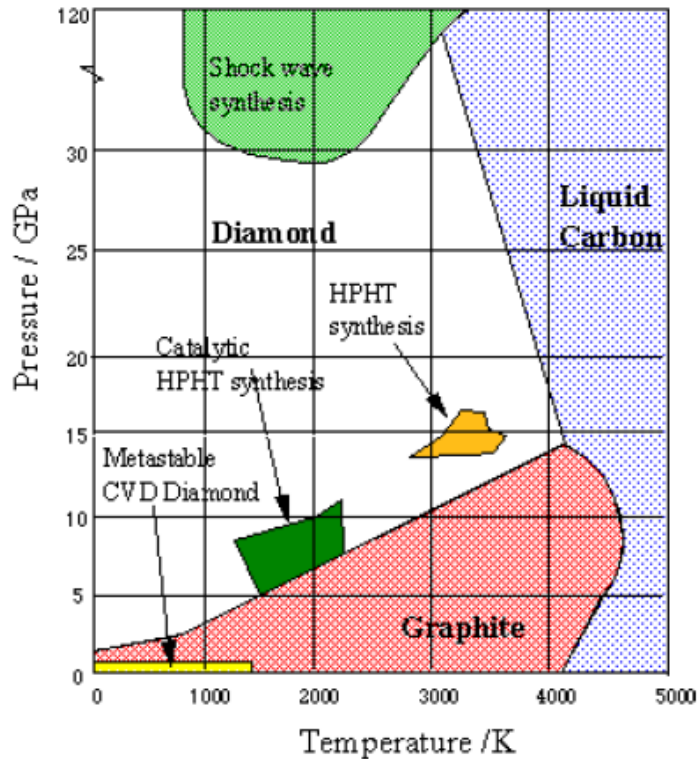


Figure 1.1 The carbon phase diagram [35] showing that diamond is a high-temperature-high-pressure carbon phase.

According to Fig. 1.1, diamond synthesis by HPHT method is easily understood. At room temperature and atmosphere pressure, diamond is metastable phase and is less stable than graphite. Therefore, the transformation from diamond to graphite exists but slowly. Under high-temperature (>75,000 atm) and high-pressure (1200~2000 °C) conditions, diamond can be synthesized successfully [32]. In the HPHT process, non-diamond carbons are solvated to produce carbons for diamond crystallization at a

pressure of 50-100 kBar and a temperature of 1,500 to 2,000 °C [40-42]. However, the size of synthesized diamond is small and the cost of high-quality diamond synthesis is high. In addition, the growth rate of diamond using HPHT method is low.

CVD method is completely different from HPHT method. To achieve CVD of diamond needs three parts: gaseous feed stock, high energy and substrates [43]. Gas feed stock must consist of at least one carbon-containing source. High energy can come from thermal, electrical, combustion or optical energy, which is used to break the gas precursors into radical species for diamond deposition [22]. So far, various CVD methods for diamond deposition under low pressure are developed, like hot filament (HF) CVD [44], direct charge (DC) arcjet-assisted CVD [45], microwave plasma-assisted CVD (MPCVD) [46], radio frequency (RF) plasma-assisted CVD [47] and combustion flame CVD [48]. The reaction mechanisms for diamond deposition within the CVD methods differ from each other. No one explanation can be used in all methods. In spite of the difference among these CVD methods, it can be concluded in several aspects [37]: 1) a gas phase must contain carbon and be activated; 2) the process of etching graphite or suppressing gaseous graphite precursors must exist; 3) the substrates are needed for nucleation and diamond growth. In summary, carbon activation, carbon transport and nucleation are the main processes in CVD. Although great efforts have been taken to study the diamond deposition process, high diamond deposition rate, high diamond quality and low cost still cannot be achieved successfully by single CVD method. MPCVD can produce high-quality diamond with a growth rate of 150 $\mu\text{m/hr}$ [49], but the cost of MPCVD is too high for applications. High-quality diamond can be obtained by HFCVD [37], but the deposition rate is as low as 0.1~10 $\mu\text{m/hr}$. Combustion flame CVD

have advantages of low cost, simple equipment, and being operated in open air [38]. However, the process of diamond deposition cannot be accurately controlled, including the diffusion of oxygen, impurities and non-diamond carbon content upon atmospheric operation, which results in low diamond quality [50].

1.3 Motivation

Diamond, as a low-compressibility material, has attracted a great number of engineers and scientists to take efforts to grow diamond films on different non-diamond substrates [22,32,51,52]. Due to its extreme properties, applications of diamond have been widely investigated as surface protection [23], optical window [24], thermal management [25], wear resistance [26], active electronic devices [27], sensors [28], acoustic speakers [29] and photons [30], and electron emitters [31]. As a semiconductor, diamond has advantages of wide band-gap, high carrier mobility, high breakdown fields, high workable temperature and negative electron affinity in microelectronics [32,33,38,39,53]. In addition, it is also attractive that diamond can work in harsh environments [53-58].

As an approach of surface coating, CVD methods satisfy the desire of diamond thin film deposition on non-diamond substrates, which make diamond thin film widely used for applications. However, there are still many challenges related to CVD methods. Due to the shortcomings of different CVD methods [55], like low deposition rate in HFCVD, poor quality in combustion flame CVD, microwave leakage in MPCVD and high heat fluxed in DCCVD and RFCVD, it is still critical and challenging to find an effective method to increase diamond film quality and deposition rate and decrease the cost of diamond synthesis.

It has been reported that chemical reactions in CVD of materials are caused by collisions of electrons, ions, atoms and molecules [53]. Therefore, it is believed that chemical reactions in CVD are critical for material synthesis. In LCVD, laser irradiation can influence chemical reactions significantly [20,21]. In this thesis work, laser

irradiation was used to affect the diamond thin film deposition process in both physical and chemical ways. With the challenges in CVD methods, a combination of laser irradiation and combustion flame CVD, laser-assisted combustion flame CVD, was applied to achieve the goal of growing high-quality, high-deposition-rate and low-cost diamond thin films. Because a great number of carbon atoms are in combustion flame and they can be excited by a light at 247.9 nm, KrF excimer laser (248 nm) is an ideal laser source for carbon atoms excitation. KrF excimer laser is also used to: 1) achieve energy coupling into combustion flame; 2) influence species proportions in the combustion flame; 3) promote seeding and nucleation process during diamond film deposition; 4) increase the diamond thin film quality and deposition rate through non-diamond carbon removal. These advantages of KrF excimer laser make diamond deposition process control feasible.

In this thesis work, efforts were conducted to explore the capability of a laser-assisted combustion flame CVD technique with KrF excimer laser irradiation for improving diamond thin film quality and deposition rate. The research efforts mainly focus on following objectives, including: 1) studying the influence of the gap distance between the inner flame and the substrates on crystallographic orientations of diamond films, diamond film quality and deposition rate to optimize the parameters for the deposition; 2) conducting *in-situ* KrF excimer laser irradiation during diamond film deposition to increase the quality and the growth rate of the diamond film with the optimal deposition parameters, which includes excimer laser irradiation on the diamond film and on the combustion flame; 3) applying *post-growth* KrF excimer laser irradiation on diamond films, which is aiming to understand and verify the effect of *in-situ* KrF

excimer laser irradiation on the diamond film during the deposition. A multi-torch combustion flame CVD was also developed for increasing the efficiency of depositing large-area diamond thin films.

1.4 Thesis outline

This thesis focuses on applying excimer laser irradiation on diamond film deposition in the open air. The whole thesis is divided into five chapters. Chapter 1 reviews the background of laser-assisted materials synthesis, diamond and diamond deposition methods and introduces the motivation and outline of this thesis. Chapter 2 investigates the effect on diamond films with changing the gap distance between the inner flame and the substrates, aiming to find out the best gap distance for growing diamond thin films. In Chapter 3, efforts were extended to apply *in-situ* KrF excimer laser irradiation during diamond film deposition. The effects of KrF excimer laser irradiation on both diamond films and combustion flame were investigated. Then the experiment of *post-growth* KrF excimer laser irradiation on diamond thin films was designed to verify and better understand non-diamond carbon removal. In Chapter 4, a multi-torch setup was developed to grow large-area diamond thin films. Chapter 5 concludes this work with key results and suggested future research directions.

References

- [1] Bass, M., *Laser Materials Processing*, Amsterdam, North-Holland (1983).
- [2] Steen, W. M., “Laser material processing—an overview”, *Journal of Optics A-Pure Applied Optics* **5**, S3 (2003).
- [3] Markevich, M. I., Podol'tsev, A. S., Piskunov, F. A., and Chao, C., “Pulsed-laser annealing of GaAs in a multilayer semiconductor structure”, *Inorganic Materials* **35**, 224 (1999).
- [4] Hatanaka, Y., Niraula, M., Nakamura, A., and Aoki, T., “Excimer laser doping techniques for II–VI semiconductors”, *Applied Surface Science* **175**, 462 (2001).
- [5] Bauerle, D., *Laser Processing and Chemistry*, 3rd Ed. Springer-Verlag Berlin, (2000).
- [6] Molian, P. A. and Waschek, A., “Laser physico-chemical vapour deposition of cubic boron nitride thin films”, *Journal of Materials Science* **28**, 1733 (1993).
- [7] Shi, J., Lu, Y. F., Chen, X. Y., Cherukuri, R. S., Mendu, K. K., Wang, H., and Batta, N., “Phase-graded deposition of diamond-like carbon on nanotips by near-field induced chemical vapor deposition”, *Applied Physics Letters* **86**, 131918 (2005).
- [8] Tsai, H. S., Chiu, H. C., Chang, S. H., Cheng, C. C., Lee, C. T., and Liu, H. P., “CO₂-Laser-Assisted Plasma-Enhanced Chemical Vapor Deposition of Silicon Dioxide Thin Film”, *Japanese Journal of Applied Physics* **40**, 3093 (2001).
- [9] Turney, W., Hung, Y. M., Starcevich, S. G., Cardinahl, P. S., Grassian, V. H., and Singmaster, K. A., “Pulsed laser-assisted chemical vapor deposition of W, Mo, and V thin films”, *Chemistry of Materials* **4**, 1192 (1992).

- [10] Tabbal, M., Meunier, M., Izquierdo, R., Beau, B., and Yelon, A., “Laser-chemical vapor deposition of W Schottky contacts on GaAs using WF₆ and SiH₄”, *Journal of Applied Physics* **81**, 6607 (1997).
- [11] Alexandrescu, R., Cireasa, R., Pugna, G., Crunteanu, A., Petcu, S., Morjan, I., Mihailescu, I. N., and Andrei, A., “CN_x thin films obtained by laser induced CVD in different gas-substrate systems”, *Applied Surface Science* **110**, 544 (1997).
- [12] Aoyagi, Y., “Beam assisted atomic layer controlled epitaxy and etching of GaAs”, *Materials Research Society Symposium Processing* **222**, 121 (1991).
- [13] Sudarsan, U., Cody, N. W., Dosluoglu, T., and Solanki, R., “Excimer laser assisted selective epitaxy of GaP”, *Applied Physics A* **50**, 325 (1990).
- [14] Donnelly, V. M., Brasen, D., Appelbaum, A., and Geva, M., “Excimer laser induced deposition of InP”, *Journal of Vacuum Science and Technology A* **4**, 716 (1986).
- [15] Irvine, S. J. C., Hill, H., Brown, G. T., Barnett, S. J., Hails, J. E., Dosser, O. D., and Mullin, J. B., “Selected area epitaxy in II–VI compounds by laser-induced photo-metalorganic vapor phase epitaxy”, *Journal of Vacuum Science and Technology B* **7**, 1191 (1989).
- [16] Fujita, Y., Fujii, S. and Iuchi, T., “Ultraviolet spectra of II–VI organometallic compounds and their application to in situ measurements of the photolysis in a metalorganic chemical vapor deposition reactor”, *Journal of Vacuum Science and Technology A* **7**, 276 (1989).

- [17] Cheng, Y. H., Qiao, X. L., Chen, J. G., Wu, Y. P., Xie, C. S., Muo, S. B., Sun, Y. B., and Tay, B. K., "Synthesis of carbon nitride films by direct current plasma assisted pulsed laser deposition", *Applied Physics a-Material* **74**, 225 (2002).
- [18] Wang, J. B., Liu, Q. X., and Yang, G. W., "Nano-crystalline diamond prepared by laser ablation solid target in liquid", *Chemical Journal of Chinese Universities* **19**, 1719 (1998).
- [19] Yang, G. W., and Wang, J. B., "Carbon nitride nanocrystals having cubic structure using pulsed laser induced liquid-solid interfacial reaction", *Applied Physics a-Materials* **71**, 343 (2000).
- [20] Ling, H., Xie, Z. Q., Gao, Y., Gebre, T., Shen, X. K., and Lu, Y. F., "Enhanced chemical vapor deposition of diamond by wavelength-matched vibrational excitations of ethylene molecules using tunable CO₂ laser irradiation", *Journal of Applied Physics* **105**, 064901 (2009).
- [21] Ling, H., Sun, J., Han, Y. X., Gebre, T., Xie, Z. Q., and Zhao, M., "Laser-induced resonant excitation of ethylene molecules in C₂H₄/C₂H₂/O₂ reactions to enhance diamond deposition", *Journal of Applied Physics* **105**, 014901 (2009).
- [22] J. Asmussen and D. K. Reinhard, *Diamond films handbook*, 1st ed. (CRC Press, 2002).
- [23] V. Shanov, W. Tabakoff, and R. N. Singh, "CVD diamond coating for erosion protection at elevated temperatures", *Journal of Materials Engineering and Performance* **11**, 220 (2002).

- [24] C. A. Klein, "Diamond windows for IR applications in adverse environments", *Diamond and Related Materials* **2**, 1024 (1993).
- [25] W. D. Brown, R. A. Beera, H. A. Naseem, and A. P. Malshe, "State-of-the-art synthesis and post-deposition processing of large area CVD diamond substrates for thermal management", *Surface & Coatings Technology* **86-87**, 698 (1996).
- [26] F. Deuerler, O. Lemmer, M. Frank, M. Pohl, and C. Hensing, "Diamond films for wear protection of hardmetal tools", *International Journal of Refractory Metals & Hard Materials* **20**, 115 (2002).
- [27] P. H. Cutler, N. M. Miskovsky, P. B. Lerner, and M. S. Chung, "The use of internal field emission to inject electronic charge carriers into the conduction band of diamond films: a review", *Applied Surface Science* **146**, 126 (1999).
- [28] P. R. Chalker and C. Johnston, "The use of internal field emission to inject electronic charge carriers into the conduction band of diamond films: a review", *Physica Status Solidi A-Applied Research* **154**, 455 (1996).
- [29] M. D. Whitfield, B. Audic, C. M. Flannery, L. P. Kehoe, G. M. Cream, C. Johnston, P. R. Chalker, and R. B. Jackman, "Polycrystalline diamond films for acoustic wave devices", *Diamond and Related Materials* **7**, 533 (1998).
- [30] E. Wu, V. Jacques, F. Treussart, H. Zeng, P. Grangier, and J. F. Roch, "Single-photon emission in the near infrared from diamond colour centre", *Journal of Luminescence* **119**, 19 (2006).
- [31] K. Okano, K. Hoshina, M. Iida, S. Koizumi, and T. Inuzuka, "Fabrication of a diamond field emitter array", *Applied Physics Letters* **64**, 2742 (1994).

- [32] F. P. Bundy, H. T. Hall, H. M. Strong, and R. H. Wentorf, "Man-made diamond", *Nature* **176**, 51 (1955).
- [33] Nazare, M. H. and Neves, A. J., *Properties, growth and applications of diamond*. INSPEC, the Institution of Electrical Engineers: London, (2001).
- [34] Davis, R. F., *Diamond films and coatings - Development, Properties, and Applications*. Noyes Publications: Park Ridge, New Jersey, (1993).
- [35] Bundy, F. P., "The P, T phase and reaction diagram for elemental carbon", *Journal of Geophysical Research* **85**, 6930 (1980).
- [36] Y. Borzdov, Y. Pal'yanov, I. Kupriyanov, V. Gusev, A. Khokhryakov, A. Sokol, and A. Efremov, "HPHT synthesis of diamond with high nitrogen content from an Fe₃N - C system", *Diamond and Related Materials* **11**, 1863 (2002).
- [37] Davis, R. F., *Diamond films and coatings - Development, Properties, and Applications*. Noyes Publications: Park Ridge, New Jersey, (1993).
- [38] Marinkovic, S. N., *Diamond synthesized at low pressure*. In *Chemistry and Physics of Carbon*, **29**, 71 (2004).
- [39] Railkar, T. A., Kang, W. P., Windischmann, H., Malshe, A. P., Naseem, H. A., Davidson, J. L., and Brown, W. D., "A Critical Review of Chemical Vapor-Deposited (CVD) Diamond for Electronic Applications", *Critical Reviews in Solid State and Materials Sciences* **25**, 163 (2000).
- [40] Sumiya H., and Toda N., "Growth of high-quality large diamond crystals under high pressure and high temperature", *Diamond and Related Materials* **5**, 1359, (1996).
- [41] Wentorf, R. H. J., "Diamond growth rates", *Journal of Physical Chemistry* **75**, 1833 (1971).

- [42] Strong, H. M. and Chrenko, R. M., "Diamond growth rates and physical properties of laboratory-made diamond", *Journal of Physical Chemistry* **75**, 1838 (1971).
- [43] B. V. Derjaguin, *Scientific American* **233**, 102 (1975).
- [44] L. Constant, C. Speisser, and F. LeNormand, *Surface Science* **387**, 28 (1997).
- [45] J. A. Smith, K. N. Rosser, H. Yagi, M. I. Wallace, P. W. May, and M. N. R. Ashfold, *Diamond and Related Materials* **10**, 370 (2001).
- [46] I. Sakaguchi, *Japanese Journal of Applied Physics Part 1-Regular Papers Brief Communications & Review Papers* **45**, 6398 (2006).
- [47] R. B. Jackman, J. Beckman, and J. S. Foord, *Materials Science and Engineering B-Solid State Materials for Advanced Technology* **29**, 216 (1995).
- [48] K. Okada, S. Komatsu, T. Ishigaki, S. Matsumoto, and Y. Moriyoshi, *Journal of Applied Physics* **71**, 4920 (1992).
- [49] Ravi, K. V., "Combustion synthesis: is it the most flexible of the diamond synthesis processes?", *Diamond and Related Materials* **4**, 243 (1995).
- [50] Petherbridge, J. R., May, P. W., and Ashfold, M. N. R., "Modeling of the gas-phase chemistry in C-H-O gas mixtures for diamond chemical vapor deposition", *Journal of Applied Physics* **89**, 5219 (2001).
- [51] D. Das and R. N. Singh, "A review of nucleation, growth and low temperature synthesis of diamond thin films", *International Materials Reviews* **52**, 29 (2007).
- [52] J. Wei and J. T. Yates, "Diamond surface chemistry", *Critical Reviews in Surface Chemistry* **5**, 1 (1995).

- [53] Hauert, R., “An overview on the tribological behavior of diamond-like carbon in technical and medical applications”, *Tribology International* **37**, 991 (2004).
- [54] Aleksov, A., Denisenko, A., Kunze, M., Vescan, A., Bergmaier, A., Dollinger, G., Ebert, W., and Kohn, E., “Diamond diodes and transistors”, *Semiconductor Science and Technology* **18**, S59 (2003).
- [55] Gurbuz, Y., Esame, O., Tekin, I., Kang, W. P., and Davidson, J. L., “Diamond semiconductor technology for RF device applications”, *Solid-State Electronics* **49**, 1055 (2005).
- [56] Kohn, E., Ebert, W., Adamschik, M., Schmid, P., and Denisenko, A., “Diamond-based MEMS devices”, *New Diamond and Frontier Carbon Technology* **11**, 81 (2001).
- [57] Auciello, O., Birrell, J., Carlisle, J. A., Gerbi, J. E., Xiao, X. C., Peng, B., and Espinosa, H. D., “Materials science and fabrication processes for a new MEMS technology based on ultrananocrystalline diamond thin films”, *Journal of Physics-Condensed Matter* **16**, R539 (2004).
- [58] Kohn, E., Adamschik, M., Schmid, P., Denisenko, A., Aleksov, A., and Ebert, W., “Prospects of diamond devices”, *Journal of Physics D-Applied Physics* **34**, R77 (2001).

CHAPTER 2

Growth of Diamond Films with Different Gap Distance

2.1 Introduction

2.2 Experiments, results and discussion

2.2.1 Growth of diamond films

2.2.2 Characterization of diamond films

2.3 Conclusions

2.1 Introduction

Diamond synthesis under low pressure has been widely studied by various CVD methods, including HFCVD, MPCVD and combustion flame CVD [1-3]. Since the combustion flame CVD of diamond was first used by Hirose and Kondo in 1988 [4], this method has been demonstrated as the most flexible CVD due to the scalable nature, low utility requirement and low costs regarding as plasma-assisted process [5]. In this thesis, our work was focused on the improvement of combustion flame CVD of diamond films using a gas mixture of $C_2H_4/C_2H_2/O_2$.

In combustion flame CVD of diamond films, various parameters can be altered to change the deposition results, such as temperature, pressure, proportions of precursors and surface conditions. Efforts have been taken to study the influence of these parameter [6,7]. In our experiment, we studied the influence of different gap distance between the inner flame and the substrate (gap distance) on diamond film deposition, including crystallographic orientations, quality and deposition rate of diamond films.

Especially, as an important aspect of diamond deposition results, the crystallographic orientations of diamond films attracted many interests. The optical, electrical, mechanical and thermal properties of diamond crystals can be determined by crystallographic orientations [8,9]. Deposition of {1 0 0}-oriented diamond films have been studied for many years, because of the superior properties of {1 0 0}-oriented diamond films over {1 1 1}- and {1 1 0}-oriented diamond films [10-13]. {1 0 0}-oriented diamond films have better mechanical properties in the terms of lower roughness and higher wear resistance than other oriented diamond films [14]. Optically, {1 0 0}-oriented films are superior to {1 1 1}-oriented diamond films, including refractive index

and extinction coefficient [14]. {1 0 0}-oriented diamond films can be successfully deposited by introducing nitrogen into the growth with biasing-enhanced nucleation [15,16]. In our experiment, by adjusting the gap distance, the diamond films were grown at different position of the flame. At different positions in the flame, the radical proportions and the temperatures [17] in the combustion flame are different. Based on this point, preferential growth of {1 0 0}-oriented diamond films can be deposited in the open air. Therefore, a series of diamond film deposition experiments were carried out to investigate the control of crystallographic orientations through combustion flame CVD method with different gap distance.

On the other hand, in this chapter, the influence of the gap distance on diamond film quality and deposition rate was also investigated. Determination of the optimal gap distance for diamond film deposition is also fundamental for the rest research work in this thesis. Therefore, the work in this chapter is also aiming to better understand the diamond thin film deposition with high quality and high growth rate.

2.2 Experiments, results and discussion

2.2.1 Growth of diamond films

Fig. 2.1 shows the experimental setup for synthesis of diamond films in the open air using combustion flame CVD system. An oxygen-acetylene torch with a 1.5 mm orifice tip was in use of generating the combustion flame. C_2H_4 , C_2H_2 and O_2 were mixed up with a volume ratio of 1:0.87:1.93. This flow rates were controlled by three mass flow controllers (B7920V, Spec-Air Gases & Technologies). Tungsten carbide plates with a dimension of $12.7 \times 12.7 \times 1.6 \text{ mm}^3$ (BS-6S, Basic Carbide Corp., containing 6% cobalt) were used as substrates for diamond thin film deposition. A cooling water system was used to cool the substrates, which was mounted on the X-Y-Z stage with motors. The substrates on the stage can be precisely controlled to an exact position. The step size of each motor was $1.25 \text{ }\mu\text{m}$, which satisfied the requirement of the gap distance control. The temperature of the substrate was monitored by a pyrometer (Omega Engineering, Inc., OS3752). The temperature of the substrate surface was kept at $760\text{-}780 \text{ }^\circ\text{C}$ by changing the flow rate of the cooling water system.

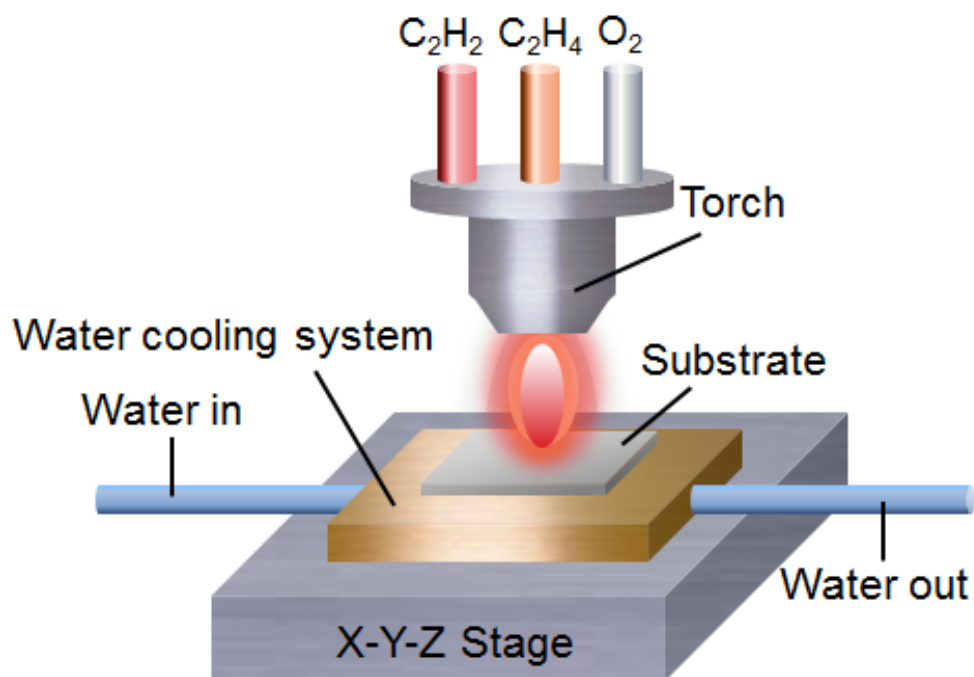


Figure 2.1 A schematic diagram of combustion flame CVD.

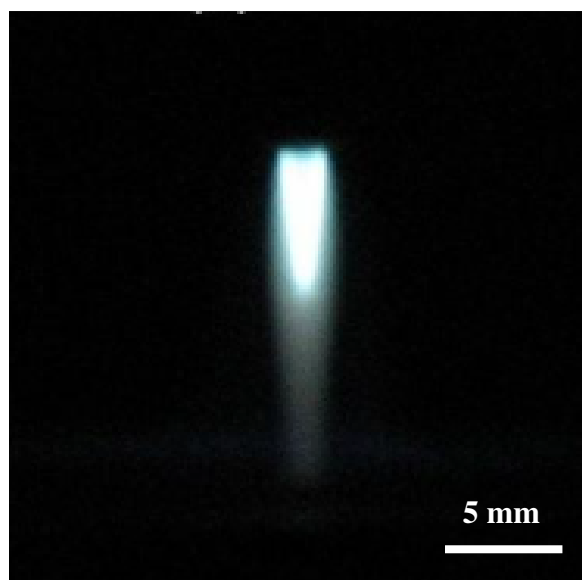


Figure 2.2 A typical optical image of the $C_2H_4/C_2H_2/O_2$ combustion flame

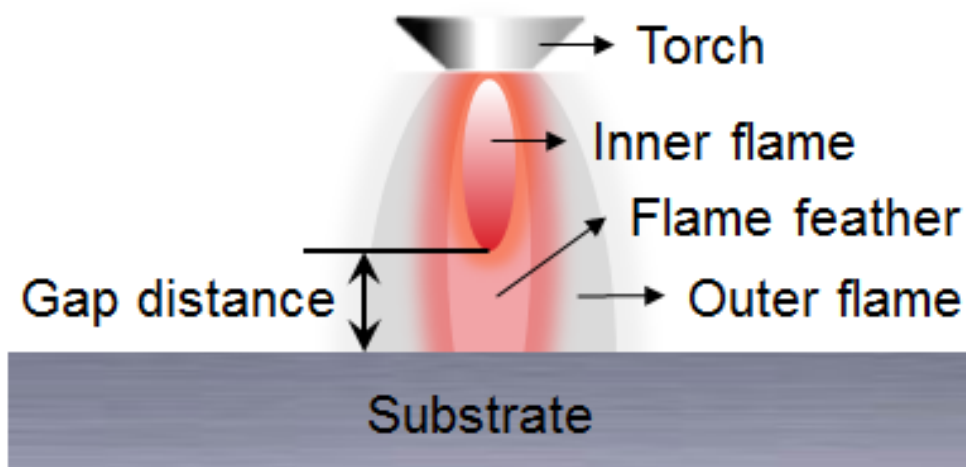


Figure 2.3 A schematic diagram showing the gap distance between the inner flame and the substrate.

Fig. 2.2 shows the optical image of the $C_2H_4/C_2H_2/O_2$ combustion flame. The inner flame was about 6 mm long and the length of the whole flame was around 12 mm. Fig. 2.3 shows the gap distance between the inner flame and the substrate. The flame is composed of the inner flame, the flame feather and the outer flame. The substrate was located in the flame feather region for diamond film growth, in which the temperature is around 3000 °C [17]. The gap distance between the inner flame and the substrate was changed from 0.2 to 0.8 mm with a step of 0.1 mm. To figure out the influence of the gap distance, diamond films were deposited under the same conditions including the deposition time, the substrate temperature and the gas flow. For each position, the diamond film was deposited for 45 min with controlling the substrate temperature at 760-780 °C. Then, diamond films were characterized by SEM and Raman spectroscopy.

2.2.2 Characterization of diamond films

Surface morphologies of the deposited diamond films were characterized by a scanning electron microscope (SEM; XL-30, Philips Electronics). Diamond film thickness of was measured by a stylus profiler (XP-2, Ambios Technology). Raman spectroscopy (inVia H 18415, Renishaw) was used to evaluate the quality of the diamond films deposited. The Raman system with a wavelength of 514.5 nm and a power of 10-20 mW laser (Innova 300, Coherent, Inc.) can be operated in a multichannel mode. The beam was focused to a spot size of 5 μm . The Raman spectrometer was calibrated by a single crystal silicon wafer before the Raman characterization of the diamond films.

Diamond morphology

Diamond films were deposited with a preferential growth at the center of the WC substrates and were grown with different gap distance from 0.2 to 0.8 mm for 45 min. As shown in Fig. 2.4, the morphologies of the diamond films varied with different gap distance. With gap distance between 0.2 and 0.3 mm, $\{1\ 0\ 0\}$ -oriented diamond films were deposited on the WC substrate, however, when the gap distance increased to 0.4-0.8 mm, $\{1\ 1\ 1\}$ -oriented diamond films were obtained. This phenomenon illustrates that the crystallographic orientations of diamond films can be controlled by the gap distance. It is also noticed that, the average size of the diamond grains decreased as the gap distance increased. This can be explained by that diamond film surface temperature is different at different positions in the flame. The surface temperature increased while the substrate was closer to the inner flame, which meant the gap distance decreased. The increase in temperature can promote the growth rate of diamond by enhancing chemical reactions on the diamond surface. As the temperature went up, the growth rate of $\{1\ 1\ 1\}$ facets were

promoted faster than that of $\{1\ 0\ 0\}$ facets, thus leading to preferentially $\{1\ 0\ 0\}$ -oriented diamond films at small gap distance. However, when the gap distance was too small, the high temperature led to oxidation or graphitization of the diamond surface. Additionally, as the growth rate increased, the average size of the diamond grains increased. Therefore, the average size of the diamond grains increased with the gap distance decreasing.

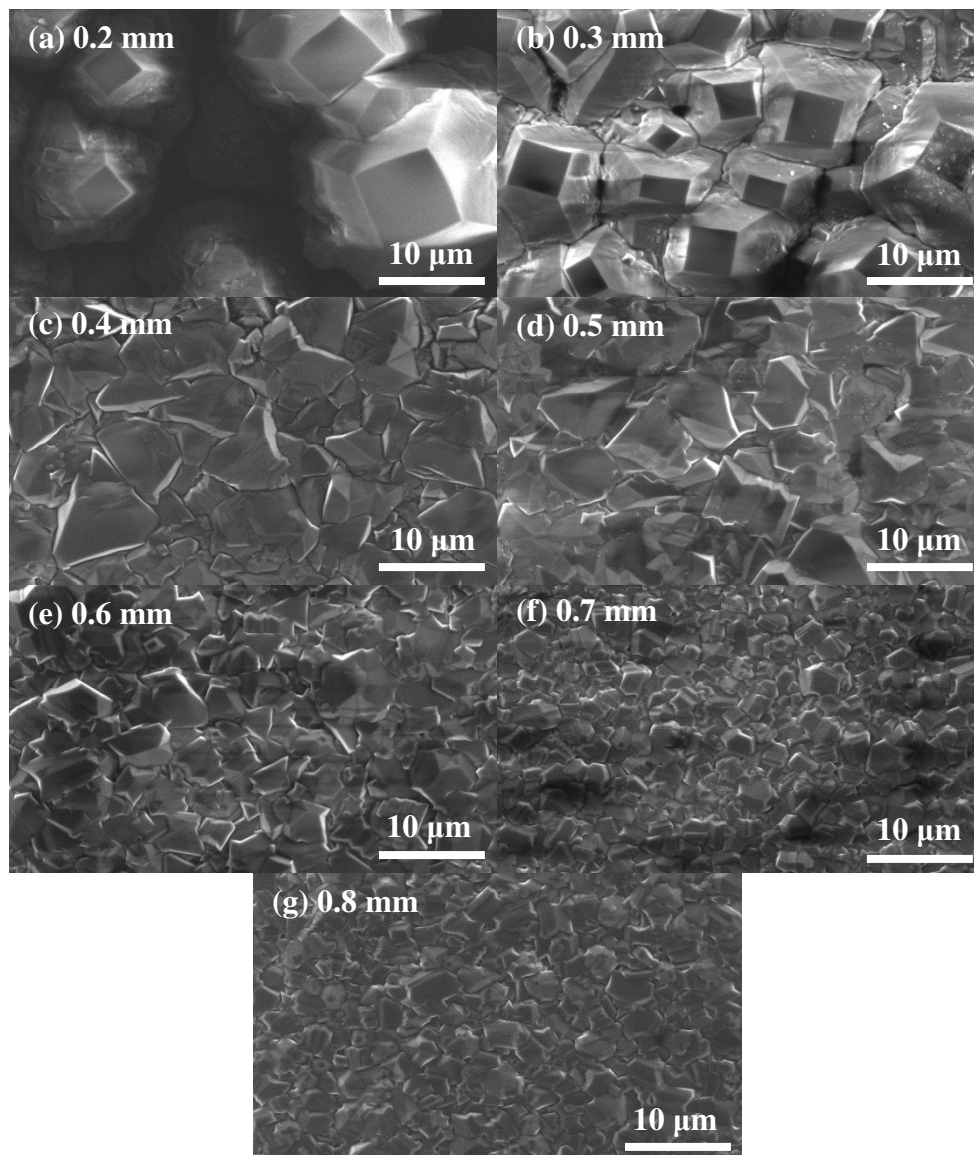


Figure 2.4 Typical SEM images of diamond films with gap distance of (a) 0.2, (b) 0.3, (c) 0.4, (d) 0.5, (e) 0.6, (f) 0.7 and (g) 0.8 mm gap distance, respectively.

Film thickness analysis

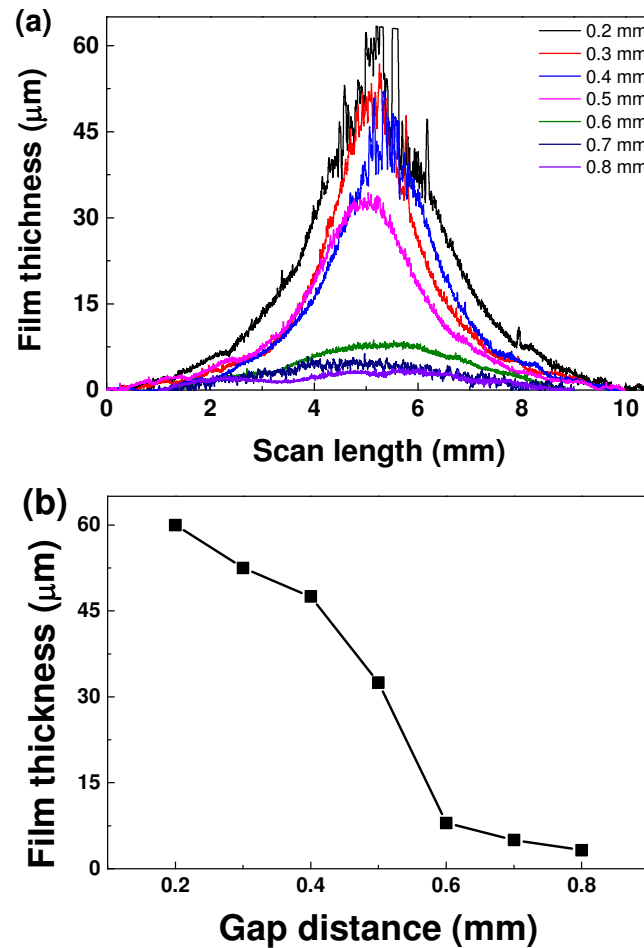


Figure 2.5 (a) Thickness of diamond films deposited with different gap distance and (b) the relationship between gap distance and film thickness.

Fig. 2.5 (a) shows thickness of the diamond films deposited at different gap distance. As Fig. 2.5 (b) shown, film thickness decreased from 60 to 6 μm with the gap distance increasing from 0.2 to 0.8 mm. Fig. 2.5 exhibits the same trend with that of the grain sizes showed in SEM images of Fig. 2.4. It can also be explained by the temperature on the diamond film surface decreased as the gap distance increased. With

the temperature decreasing, the growth rate of the diamond film decreased. Thus, the film thickness decreased with gap distance increasing.

Raman analysis of deposited diamond films

Fig. 2.6 (a) shows the Raman spectra of the diamond films deposited with different gap distance from 0.2 to 0.8 mm. Raman spectroscopy was used to evaluate the phase purity of the diamond films deposited. Sharp diamond peaks around 1332 cm^{-1} and broad G-bands around 1500 cm^{-1} were observed. When the gap distance was between 0.2 and 0.4 mm, the Raman spectra of the diamond films exhibit weak diamond peaks and relatively strong G-bands. While the gap distance was between 0.5 and 0.8 mm, the diamond peaks became stronger and the intensity of G-bands decreased. Low ratio of the intensity of diamond peak and G-band illustrates the low diamond quality due to defects, impurities and non-diamond carbon contents. The diamond quality is evaluated by the diamond quality factor, which was calculated by the function of

$$Q_{diamond} = \frac{I_{diamond\ peak}}{I_{diamond\ peak} + \frac{I_{carbon-bonds}}{233}} \times 100\% [18].$$

As shown in Fig. 2.6 (b), the diamond quality increased as the gap distance increased from 0.2 to 0.5 mm. When the gap distance was between 0.5 and 0.8 mm, the diamond quality increased slightly.

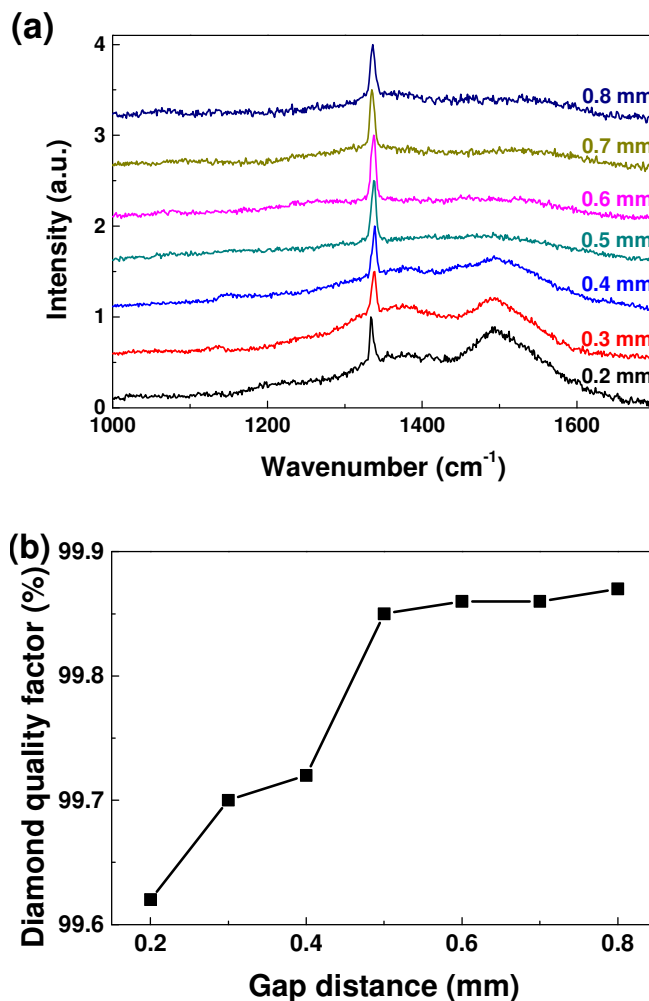


Figure 2.6 (a) Typical Raman spectra of diamond films deposited with different gap distance and (b) the relationship between gap distance and diamond quality factor.

As we discussed above, temperature on the diamond film surface played an important role in diamond deposition. It has a dramatic effect on major properties, including morphology and growth rate of diamond film. As well as these two properties, diamond quality is influenced significantly by the diamond film surface temperature. As the gap distance decreased, the temperature increased, leading to the decrease of diamond film quality, due to a potential oxidation or graphitization of the diamond surface.

2.3 Conclusions

Different gap distance between the inner flame and the substrate using a combustion flame CVD technique was studied to modify the morphologies of diamond films, improve the diamond quality and increase the diamond deposition rate.

With the gap distance between 0.2-0.3 mm, {1 0 0}-oriented diamond films were deposited, however, when the gap distance increased to 0.4-0.8 mm, {1 1 1}-oriented diamond films were obtained. This suggests an easy method to control crystallographic orientations.

On the other hand, thickness of the diamond films measured by a stylus profiler indicates that deposition rate became faster as the gap distance got smaller. Raman spectra of the diamond films deposited with different gap distance shows that high-quality diamond films can be synthesized with the gap distance between 0.5-0.8 mm. It is believed that the optimal gap distance for depositing {1 0 0}-oriented diamond film with relatively high quality and large thickness is 0.3 mm. The optimal gap distance for {1 1 1}-oriented diamond films is 0.5 mm. Therefore, the optimal gap distance of 0.5 mm was applied in other experiments in this thesis.

References

- [1] Haubner, R. and Lux, B. “Diamond growth by hot-filament CVD: State of the art”, *Diamond and Related Materials* **2**, 1277 (1993).
- [2] McCauley, T. S., and Vohra, Y. K., “Homoepitaxial diamond film deposition on a brilliant cut diamond anvil”, *Applied Physics Letters* **66**, 1486 (1995).
- [3] Eguchi, K., Yata, S., and Yoshida, T., “Uniform and large-area deposition of diamond by cyclic thermal plasma chemical vapor deposition”, *Applied Physics Letters* **64**, 58 (1994).
- [4] Hirose, H. and Komaki, K. Eur. Pat. Appl. EP324538 (1988).
- [5] Ravi, K. V., “Combustion synthesis: is it the most flexible of the diamond synthesis processes?”, *Diamond and Related Materials* **4**, 243 (1995).
- [6] T. Le Huu, H. Zaidi, and D. Paulmier, *Thin Solid Films* **308**, 147 (1997).
- [7] T. Le Huu, M. Schmitt, D. Paulmier, A. G. Mamalis, and A. Grabchenko, *Wear* **229**, 843 (1999).
- [8] Liu, T., Raabe, D., Mao, W., and Zaefferer, S. “Microtexture and Grain Boundaries in Freestanding CVD Diamond Films: Growth and Twinning Mechanisms”, *Advanced Functional Materials* **19**, 3880 (2009).
- [9] Butler, J. E. and Oleynik, I. “A mechanism for crystal twinning in the growth of diamond by chemical vapour deposition”, *Philosophical Transactions of the Royal Society A* **366**, 295 (2008).
- [10] Ayres, V. M., Bieler, T. R., Kanatzidis, M. G., Spano, J., Hagopian, S., Balhareth, H., Wright, B. F. Farhan, M., Abdul Majeed, J., Spach, D, Wright, B. L., and

- Asmussen, J., "The effect of nitrogen on competitive growth mechanisms of diamond thin films", *Diamond and Related Materials* **9**, 236 (2000).
- [11] Schade, A., Rosiwal, S. M., and Singer, R. F., "Influence of surface topography of HF-CVD diamond films on self-mated planar sliding contacts in dry environments", *Diamond and Related Materials* **15**, 1682 (2006).
- [12] Avigal, Y., Glozman, O., Etsion, I., Halperin, G., and Hoffman, A., "[100]-Textured diamond films for tribological applications", *Diamond and Related Materials* **6**, 381 (1997).
- [13] Su, Q. F. , Xia, Y. B., Wang, L. J. , Liu ,J. M., and Shi, W. M., "Influence of texture on optical and electrical properties of diamond films", *Vacuum* **81**, 644 (2007).
- [14] Grigoryev, E. V., Savenko, V. N., Sheglov, D. V., Matveev, A. V., Cherepanov, V. A., and Zolkin, A. S., "Synthesis of diamond crystals from oxygen-acetylene flames on a metal substrate at low temperature", *Carbon* **36**, 581 (1998).
- [15] Stoner, B. R., Sahaida, S. R., Bade, J. P., Southworth, P., and Ellis, P. J., "Highly oriented, textured diamond films on silicon via bias-enhanced nucleation and textured growth", *Journal of Materials Research* **8**, 1334 (1993).
- [16] Fox, B. A., Stoner, B. R., Malta, D. M., Ellis, P. J., Glass, R. C., and Sivazlian, F. R., "Epitaxial nucleation, growth and characterization of highly oriented, (100)-textured diamond films on silicon", *Diamond and Related Materials* **3**, 382 (1994).
- [17] X. N. He, X. K. Shen, T. Gebre, Z. Q. Xie, L. Jiang, and Y. F. Lu, "Spectroscopic Determination of Rotational Temperature in $C_2H_4/C_2H_2/O_2$ Flames for Diamond Growth with and without Tunable CO_2 Laser Excitation", *Applied Optics*, **49**, 1555 (2010).

- [18] Stephanie R. Sails, Derek J. Gardiner, Michael Bowden, James Savage and Don Rodway, "Monitoring the quality of diamond films using Raman spectra excited at 514.5 nm and 633 nm", *Diamond and Related Materials*, Volume **5**, 589 (1996).

CHAPTER 3

In-situ Excimer Laser Irradiation during Diamond Film Deposition

3.1 Introduction

3.2 Experiments, results and discussion

3.2.1 Excimer laser irradiation on the diamond film

3.2.2 Excimer laser irradiation on the flame

3.2.3 Post-growth excimer laser irradiation on diamond films

3.3 Conclusions

3.1 Introduction

Diamond film deposition has a great value for industrial application and scientific research, because diamond films have great mechanical properties like solidness and high wear-resistance, high thermal conductivity, large band gap, low infrared absorption and great optical properties [1]. Since the invention of the combustion flame CVD of diamond by Hirose and Kondo in 1988 [2], great efforts were made to improve this method in order to promote the diamond quality and the uniformity of the diamond films. Through the adjustment of the deposition conditions, including temperature, species proportions and surface conditions [3], diamond quality can be controlled.

Laser energy can be coupled into combustion flame CVD to influence the deposition conditions [4,5]. Previously, applying a wavelength-tunable CO₂ laser was promoted to improve the flame deposition conditions through multi-energy processing (MEP) in LANE [4,5]. In C₂H₄/C₂H₂/O₂ flame, the frequencies of molecular vibrations are in the infrared (IR) range, which matches one wavelength (10.532 μm) of the laser. Therefore, MEP was used to promote and control chemical reactions in combustion flame CVD by resonant vibrational excitation of the ethylene molecules in C₂H₄/C₂H₂/O₂ flame [4,5].

On the other hand, many substrate surface pretreatments can influence the deposition conditions as well, including scratching [6-8], seeding [3,8,9], laser pretreatment [9-11], plasma pretreatment [12,13], ion implantation [14-17], and chemical pretreatment [6,18,19].

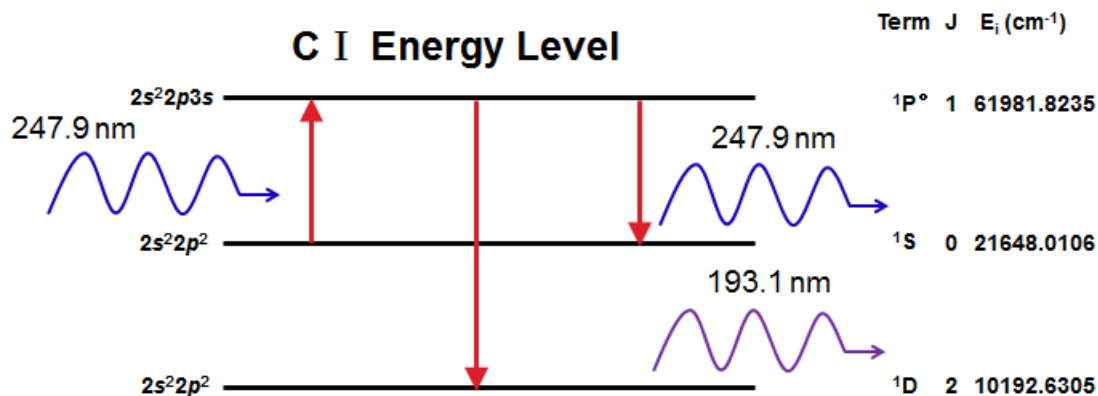


Figure 3.1 A schematic diagram showing electron excitation of carbon atoms

To influence the deposition conditions, a krypton fluoride (KrF) excimer laser was introduced to the combustion flame CVD of diamond films. The KrF excimer laser is a nanosecond pulsed laser, which is significantly different from the CO₂ continuous-wave laser. Due to the fact that a number of carbon atoms contained in combustion flame can be electronically excited by a light at 247.9 nm (Fig. 3.1), KrF excimer laser (248 nm) is an ideal laser source for carbon atoms excitation. KrF excimer laser can be used to: 1) achieve energy coupling into combustion flame; 2) influence species proportions in the combustion flame; 3) promote seeding and nucleation process during diamond film deposition; 4) increase the diamond thin film quality and deposition rate through non-diamond carbon removal. These advantages of KrF excimer laser makes diamond deposition process control feasible.

Based on these advantages, three parts are involved into the study of the effect of KrF excimer laser irradiation during diamond film growth. One is that the excimer laser was introduced with an angle of 30° to the diamond film during the deposition, aiming to influence the seeding and nucleation by laser irradiation. The second one is that the

excimer laser was introduced in parallel to the substrate to irradiate the flame during the deposition process, in order to investigate the influence of excimer laser irradiation on the flame, and eventually the influence on diamond film quality and deposition rate. The last one is *post-growth* KrF excimer laser irradiation on diamond films, which is used to verify and understand the effect of KrF excimer laser irradiation on diamond films.

The objective of these experiments was to understand the effects of the excimer laser irradiation on the diamond film growth, including diamond quality and deposition rate. Additionally, developing an efficiency method to realize non-diamond carbon removal is also valuable for further research investigation. In this chapter, we mainly focused on experimental study of *in-situ* KrF excimer laser irradiation during diamond film deposition. Fundamental understanding needs further theoretical simulations in the future.

3.2 Experiments, results and discussion

In this chapter, two experimental setups were used, because the KrF excimer laser was introduced to the diamond film deposition in two different ways. One is that the excimer laser was used to irradiate the diamond films during the diamond film deposition, where the excimer laser beam has an angle of 30° with the substrates. The other one is that the KrF excimer laser was introduced in parallel to the substrates to irradiate the $C_2H_4/C_2H_2/O_2$ combustion flame. The KrF excimer laser (COMPexPro 205, Lambda Physik) applied in the experiments was a nanosecond pulsed laser with a pulse width of 23 ns. The wavelength of the KrF excimer laser is 248 nm. The frequency of the excimer laser was tunable, from 1 to 51 Hz. Two operation modes of the KrF excimer laser can be used, internal mode and external mode. The excimer laser was introduced to the diamond film deposition under the internal mode.

3.2.1 Excimer laser irradiation on the diamond film

Fig. 3.2 shows a schematic diagram of the experimental setup for diamond film deposition with excimer laser irradiation on the diamond film in the open atmosphere. A torch was used to generate the $C_2H_4/C_2H_2/O_2$ combustion flame. The diameter of the orifice of the torch was 1.5 mm. C_2H_4 , C_2H_2 and O_2 were mixed up with a volume ratio of 1:0.87:1.93. This flow rates were controlled by three mass flow controllers (B7920V, Spec-Air Gases & Technologies). The WC substrates (BS-6S, Basic Carbide Corp., containing 6% cobalt) were placed on the water cooling system which was fixed on an X-Y-Z stage with motors. The temperature of the substrate surface was monitored by a pyrometer (Omega Engineering, Inc., OS3752) and was controlled at 760 to 780 °C by controlling the water flow in the cooling system. The 248 nm KrF excimer laser was used

in the diamond film deposition to irradiate the diamond film. The excimer laser was fixed with an angle of 30° to the substrate and the $2 \times 2 \text{ cm}^2$ laser beam can cover the whole circle deposition area on the substrate with a diameter of 9 mm. The fluence of the excimer laser was varied with a range of $52.8\text{--}85 \text{ mJ/cm}^2$. The excimer laser frequency was set to 1 Hz. Diamond films were grown on the WC substrates for 30 min. The gap distance was fixed at 0.5 mm.

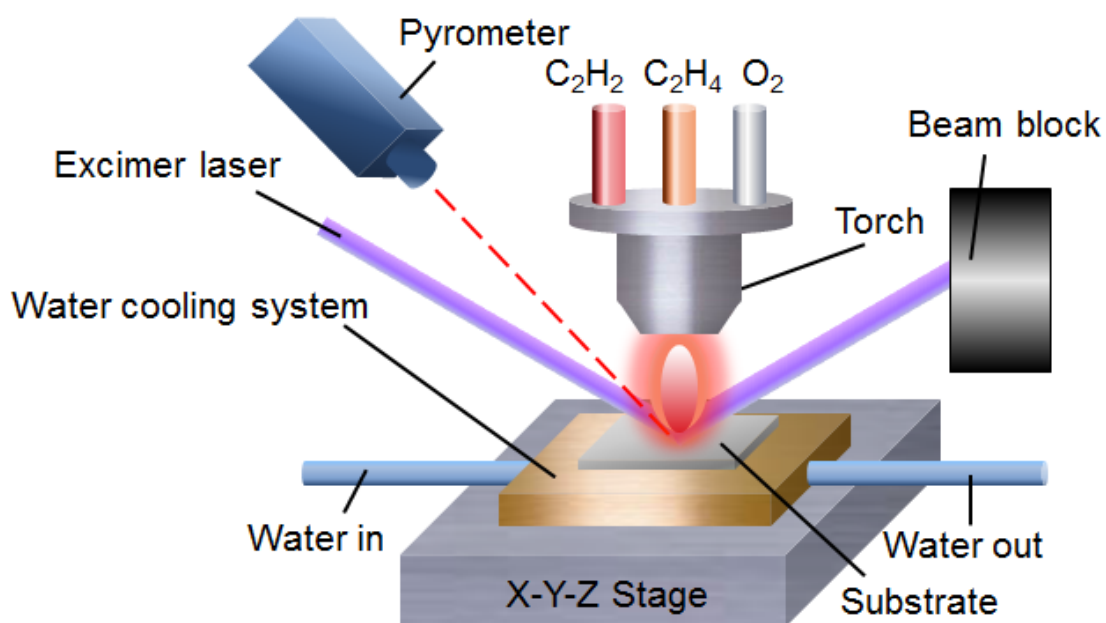


Figure 3.2 A schematic diagram showing the experimental setup for diamond films deposited using KrF excimer laser irradiation on the diamond film.

A scanning electron microscope (SEM; XL-30, Philips Electronics) was used to characterize the morphologies of the diamond films. The thickness of the diamond films was measured by a stylus profiler (XP-2, Ambios Technology). Raman spectroscopy (inVia H 18415, Renishaw) was used to evaluate the quality of the diamond films

deposited. The Raman system has a wavelength of 514 nm, power of 100 mW argon ion laser (Innova 300, Coherent, Inc.). To avoid the damage to the samples and produce efficient Raman excitation, the power of the argon ion laser was set to 10-20 mW. Raman spectrometer was calibrated by a single crystal silicon wafer before the Raman characterization of the diamond films.

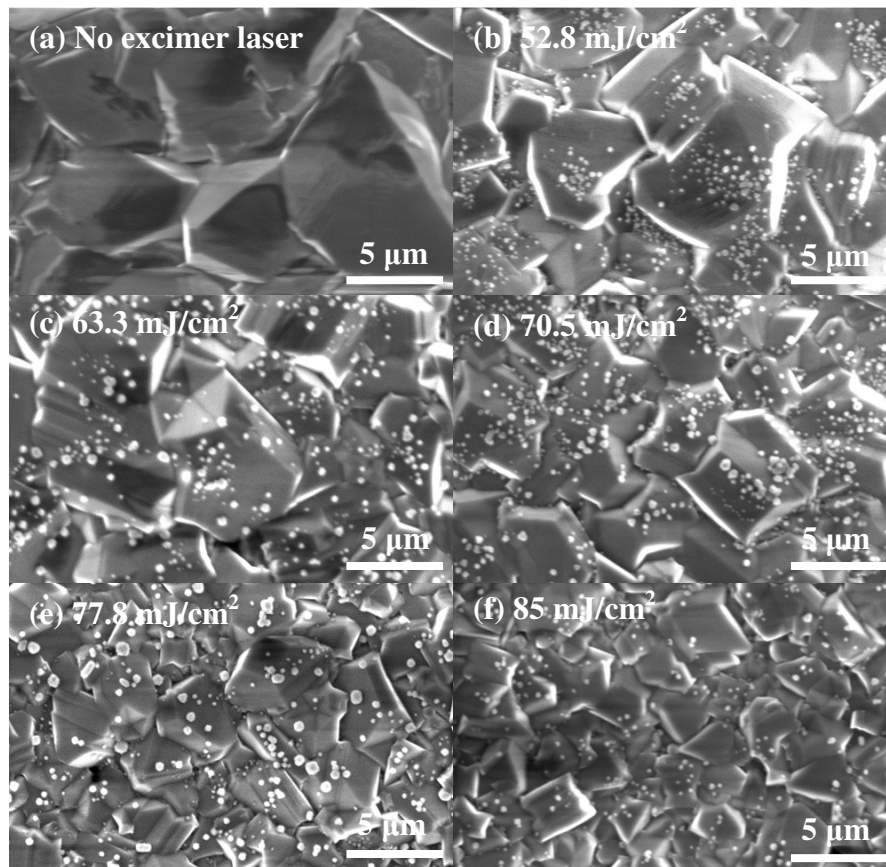


Figure 3.3 Typical SEM images of diamond films deposited (a) without excimer laser, with excimer laser irradiation at fluences of (b) 52.8, (c) 63.3, (d) 70.5, (e) 77.8 and (f) 85 mJ/cm², respectively.

Diamond films were grown for 30 min on the WC substrates with different fluences of the excimer laser. SEM images were used to study the morphologies of the diamond films, as shown in Fig. 3.3. It is observed that all diamond films consisted of polycrystalline grains. Compared to those deposited with excimer laser irradiation, the diamond film deposited without excimer irradiation had larger crystal size. Moreover, Fig. 3.3 (b)-(f) shows that the average size of the diamond crystals decreased with the excimer laser fluence increased. This phenomenon can be explained by that excimer laser could create crystalline defects on diamond film surface. These defects could change the surface conditions of the diamond films by serving as new sites for secondary nucleation during the deposition process. As the fluence of the excimer laser increasing, the crystalline defect generation rate increased. More new secondary nucleation sites were generated. Since gas flow gate was fixed, the carbon source was unchanged. New diamond grains were grown at these new sites, thus led to smaller average size. Therefore, the average size of the diamond crystals decreased as the fluence of the excimer laser increased.

Thickness of the diamond films deposited with excimer laser irradiation at different laser fluences on the WC substrates was measured by a stylus profiler, as shown in Fig. 3.4 (a). Fig. 3.4 (b) shows the relationship between the thickness of the diamond films and the fluence of the excimer laser. Diamond film thickness increased from 14 to 22 μm as the excimer laser fluence increased from 0 to 70.5 mJ/cm^2 . With the fluence increasing to 85 mJ/cm^2 , the diamond film thickness decreased to 6 μm . These changes in film thickness reflected changes in diamond film deposition rate.

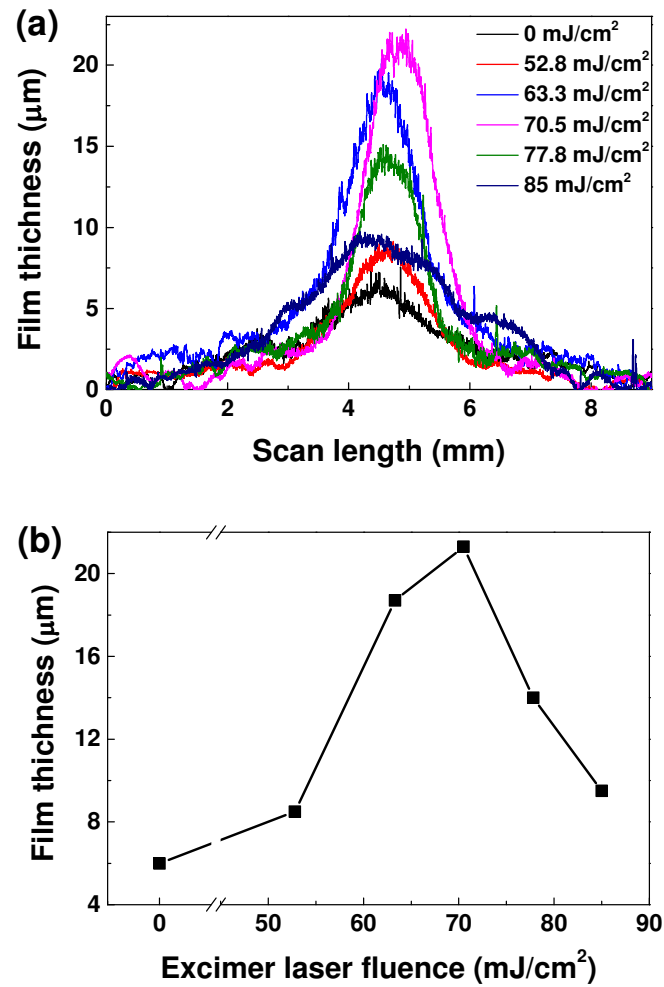


Figure 3.4 (a) Thickness of diamond films deposited with excimer laser irradiation at different laser fluences on the diamond films and (b) the relationship between laser fluence and film thickness.

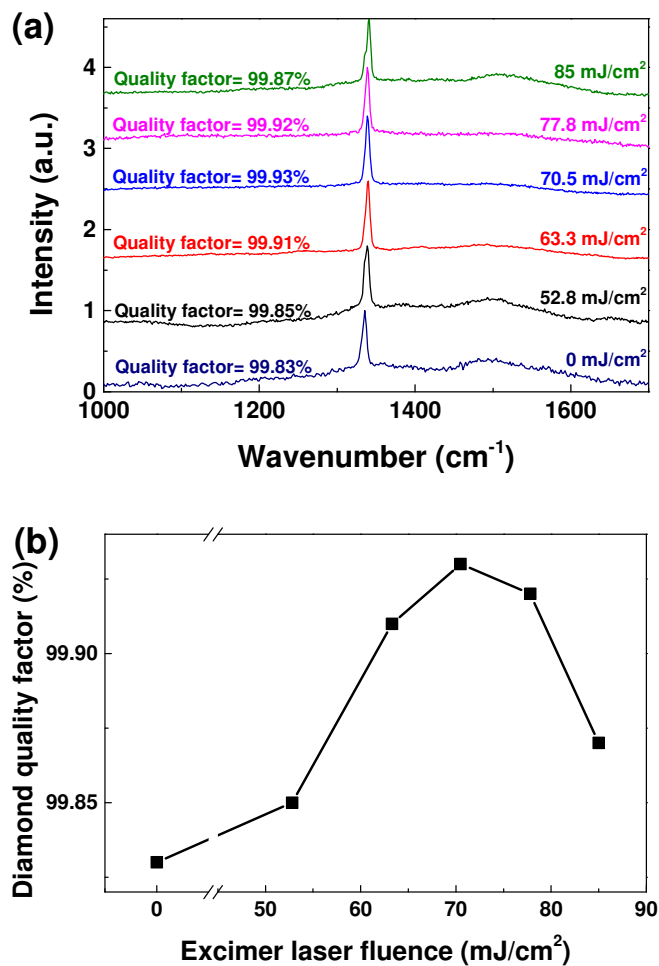


Figure 3.5 (a) Typical Raman spectra of diamond films deposited with excimer laser irradiation at different laser fluences on the diamond films and (b) the relationship between laser fluence and diamond quality factor.

The quality of diamond film was characterized by a Raman system. Fig. 3.5 (a) shows the Raman spectra of the diamond films deposited with excimer laser irradiation at different fluences on the diamond films. The diamond quality was evaluated by the diamond quality factor, which was calculated by the function

$$Q_{diamond} = \frac{I_{diamond\ peak}}{I_{diamond\ peak} + \frac{I_{carbon-bonds}}{233}} \times 100\% [20].$$

Carbon-bands includes D-bands related to disordered carbon structure around 1360 cm^{-1} and G-bands around 1500 cm^{-1} . G-bands stand for amorphous carbon which corresponded to sp^2 graphitic phase. Sharp diamond peaks (sp^3 diamond hybridization-bond) are observed at around 1332 cm^{-1} . It is observed that the G-bands intensities were changing with the fluence of the excimer laser, which indicates that the purity of diamond sp^3 bonding was changing. As shown in Fig. 3.5 (b), the same trend with Fig. 3.4 (b) was observed. With the excimer laser fluence increased from 0 to 70.5 mJ/cm^2 , the diamond film quality increased. Then the quality of the diamond films decreased as the fluence increased to 85 mJ/cm^2 .

Ultra-short pulsed laser irradiation can lead to transformation of diamond to more stable graphite [21]. Therefore, with excimer laser irradiation on diamond film during the deposition process, the sp^3 carbon atoms on the film surface were graphitized to sp^2 bonding, while the already existing non-diamond carbon was partially removed. Additionally, the crystalline defects of diamond were also produced by excimer laser irradiation. The diamond defects and parts of the sp^2 carbon atoms generated by excimer laser irradiation formed new sites for secondary nucleation. Graphitization of diamond film surface led to a decrease of both diamond film quality and deposition rate. On the other hand, these two diamond film properties were increased by non-diamond carbon removal and the continuously secondary nucleation respectively. With increasing excimer laser fluence, these three processes were all accelerated, but the increase of graphitization was higher than that of non-diamond carbon removal and secondary nucleation. With relatively low excimer laser fluence, the two processes of non-diamond carbon and secondary nucleation dominated in the diamond film deposition, which resulted in an

increased of diamond film quality and growth rate. With relatively high excimer laser fluence, graphitization prevailed in the diamond film deposition, which led to a decrease of diamond film quality and deposition rate. In session 3.2.3, this process will be further verified by the experiment of *post-growth* excimer laser irradiation on diamond film.

3.2.2 Excimer laser irradiation on the flame

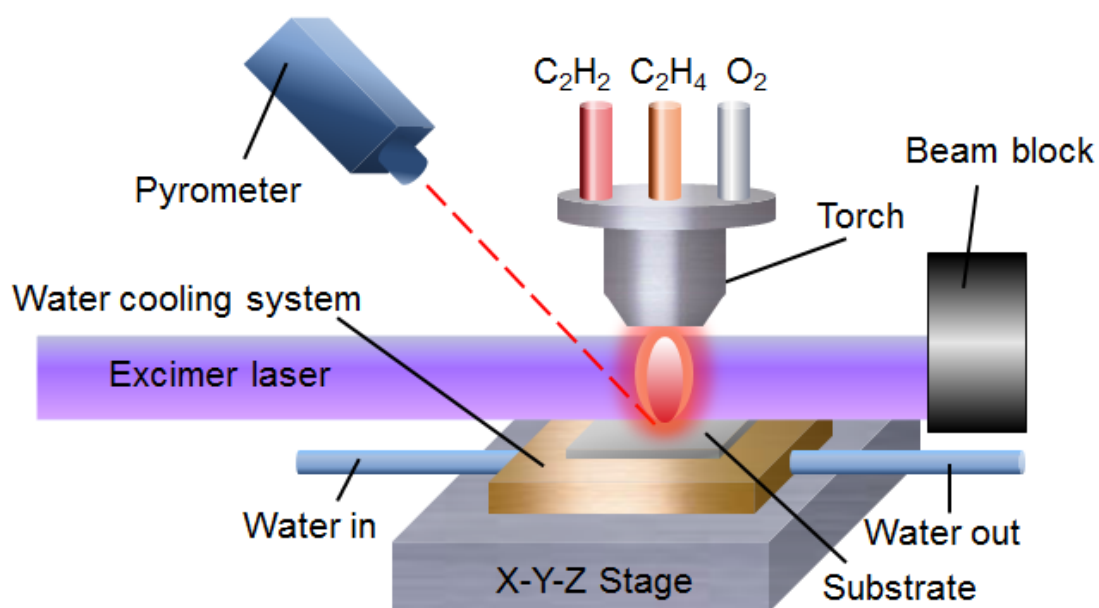


Figure 3.6 A schematic diagram showing the experimental setup for diamond film deposition with KrF excimer laser irradiation on the combustion flame.

Fig. 3.6 shows a schematic diagram of the experimental setup for diamond film deposition with excimer laser irradiation on the flame in the open air. A 248 nm KrF excimer laser was used in the diamond film deposition to irradiate the combustion flame. The excimer laser was in parallel to the substrates and normal to the flame. In addition, the $1 \times 2 \text{ cm}^2$ laser beam spot can cover the whole inner flame of the combustion flame,

because the length of the whole flame was around 12 mm and the inner flame was about 6 mm long as shown in Fig. 2.2. Moreover, the temperature of the substrate surface was monitored by a pyrometer (Omega Engineering, Inc., OS3752) and was controlled at 760 to 780 °C by controlling the water flow in the cooling system. The gap distance was fixed at 0.5 mm.

This series of the experiments was divided to two parts. In the first part, different excimer laser fluences irradiation on the flame during the diamond film deposition was applied. The fluence of the excimer laser (per pulse) was varied in a range of 105.5-229 mJ/cm² with a fixed frequency of 15 Hz. In the second part, excimer laser frequency irradiation on the flame at different frequencies during the diamond film deposition was introduced. The excimer laser frequency was changed from 1 to 35 Hz while the fluence was set to 170 mJ/cm².

3.2.2.1 Excimer laser irradiation at different laser fluences

Diamond films were grown for 30 min on the WC substrates with different fluences of the excimer laser and fixed frequency of 15 Hz. Fig. 3.7 shows the SEM images of the morphologies of the diamond films. It is observed that the average size of the diamond crystals increased with the fluence of the excimer laser increasing. It was also noticed that the size of the diamond grains deposited with excimer laser irradiation on the combustion flame became bigger than those deposited without excimer laser irradiation.

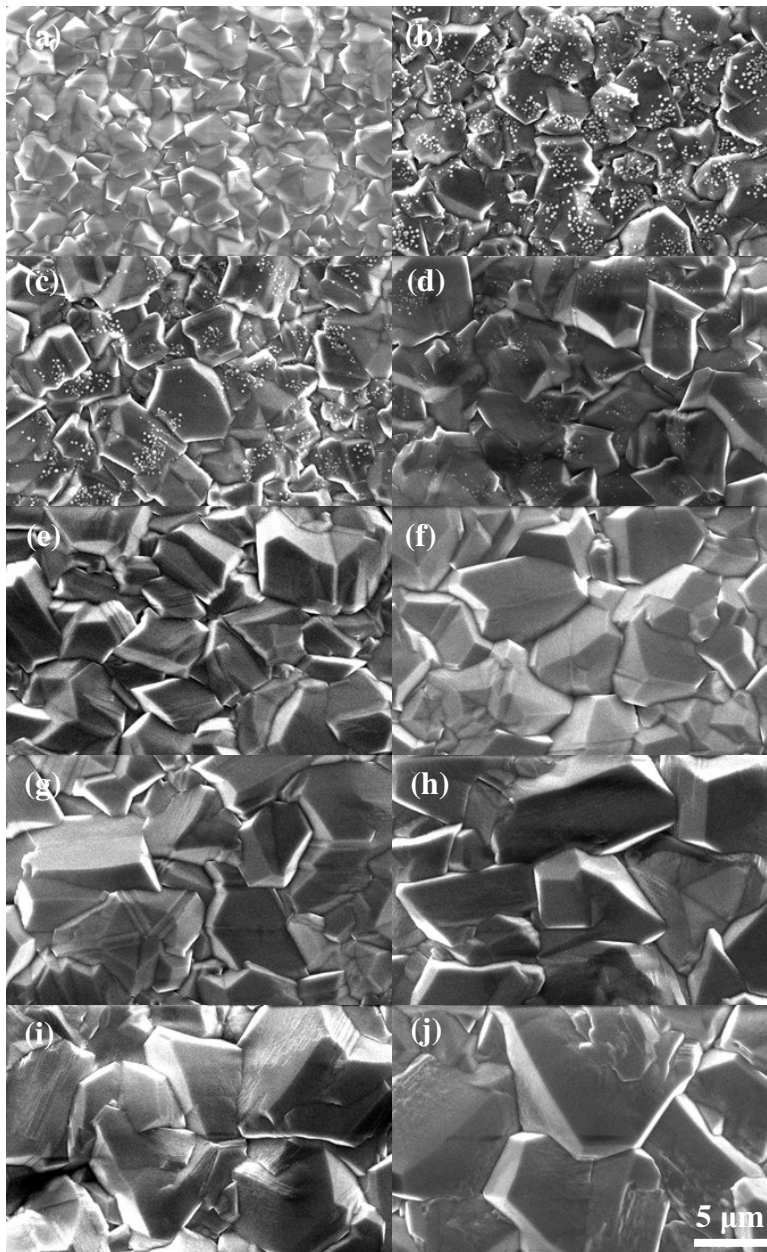


Figure 3.7 Typical SEM images of diamond films deposited (a) without excimer laser irradiation on the flame, and with excimer laser irradiation at fluences of (b) 105.5, (c) 126.5, (d) 141, (e) 155.5, (f) 170, (g) 185, (h) 199.5, (i) 214 and (j) 229 mJ/cm^2 , respectively.

The morphologies of the diamond films are related to substrate surface conditions, temperature and species proportion. In this experiment, the surface conditions of the substrates maintained the same. In addition, the temperature on the diamond film surface was fixed due to the fixed gap distance. Therefore, the species proportions in the combustion flame were influenced by *in-situ* excimer laser irradiation with electron excitation of carbon atoms. As the carbon atoms were electronically excited, the chemical reactions on the diamond surface were enhanced so it was easier to form sp^3 bonding, which led to an increase of growth rate but a decrease of the number of secondary nucleation sites. Thus, larger diamond crystals were grown. With the excimer laser fluence increasing, the number of carbon atoms excited increased. This induced that diamond film deposition rate increased and the number of secondary nucleation sites decreased as the excimer laser fluence increased. Therefore, the average size of the diamond grains increased.

Thickness of the diamond films deposited with excimer laser irradiation at different laser fluences on the WC substrates were measured by a stylus profiler as shown in Fig. 3.8 (a). Fig. 3.8 (b) shows the relationship between the thickness of the diamond films and the fluence of the excimer laser. Diamond film thickness increased from 9 to 21 μm as the excimer laser fluence increased from 105.5 to 229 mJ/cm^2 . Additionally, with excimer laser irradiation on the combustion flame, the deposited diamond films were thicker than that without excimer laser irradiation. The deposition rate of the diamond films was increasing with the excimer laser fluence increasing.

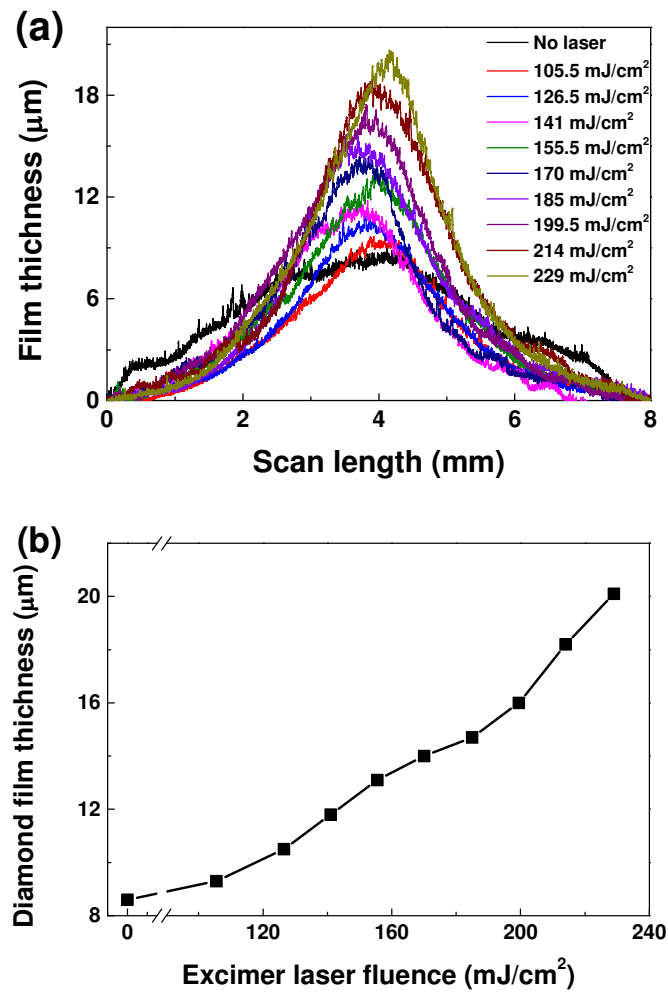


Figure 3.8 (a) Thickness of diamond films deposited with excimer laser irradiation at different laser fluences on the flame and (b) the relationship between laser fluence and film thickness.

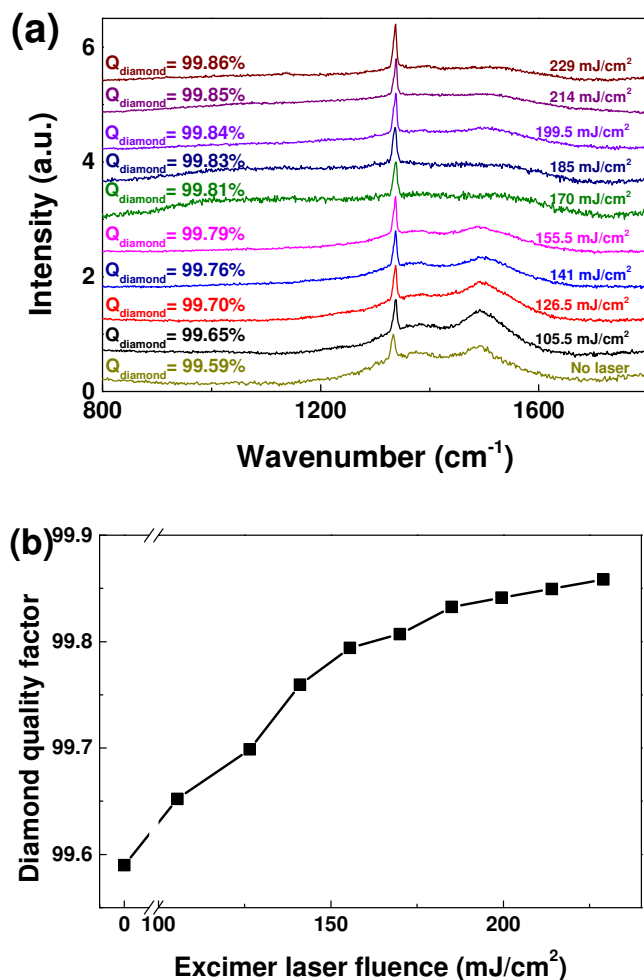


Figure 3.9 (a) Typical Raman spectra of diamond films deposited with excimer laser irradiation at different laser fluences on the flame and (b) the relationship between laser fluence and diamond quality factor.

The diamond film quality was characterized by a Raman system. Fig. 3.9 (a) shows the Raman spectra of the diamond films deposited with excimer laser irradiation on the flame at different laser fluences. Sharp diamond peaks are observed at around 1332 cm^{-1} . G-bands around 1500 cm^{-1} stand for amorphous carbon. It is also obvious that the G-bands decreased with the fluence of the excimer laser increasing, which indicates

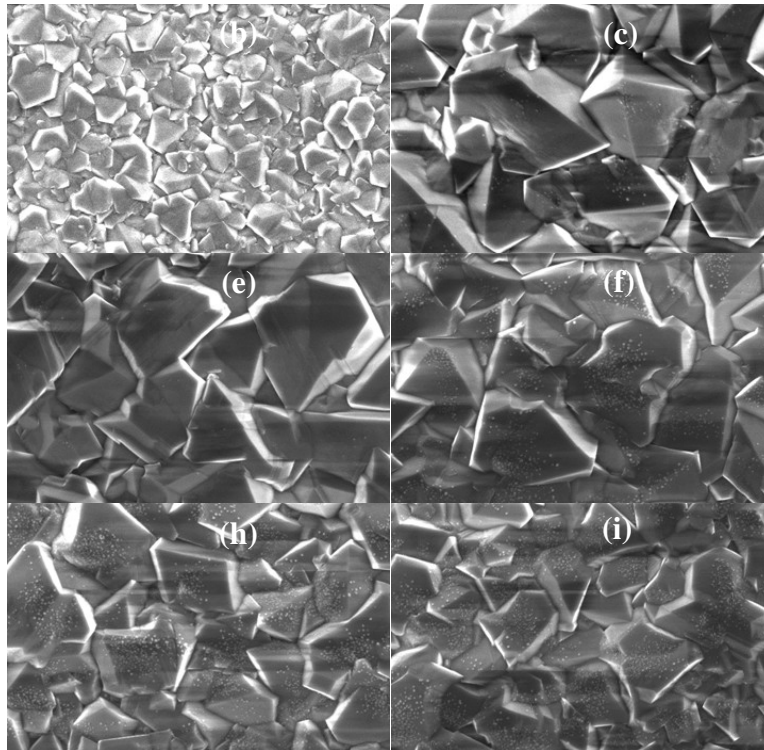
that sp^2 carbon atoms decreased. The diamond quality was evaluated by the diamond quality factor, which was calculated by the function

$$Q_{diamond} = \frac{I_{diamond\ peak}}{I_{diamond\ peak} + \frac{I_{carbon-bonds}}{233}} \times 100\% [20].$$

As shown in Fig. 3.9 (b), with the the excimer laser fluence increased from 105.5 to 229 mJ/cm^2 , the diamond film quality increased.

Grain boundaries constituted preferential locations for impurities incorporation. With fluence increasing, the diamond grain sizes increased. Therefore, imperfections such as grain boundaries decreased, which led to an increase of diamond phase purity.

3.2.2.2 Excimer laser irradiation at different frequencies



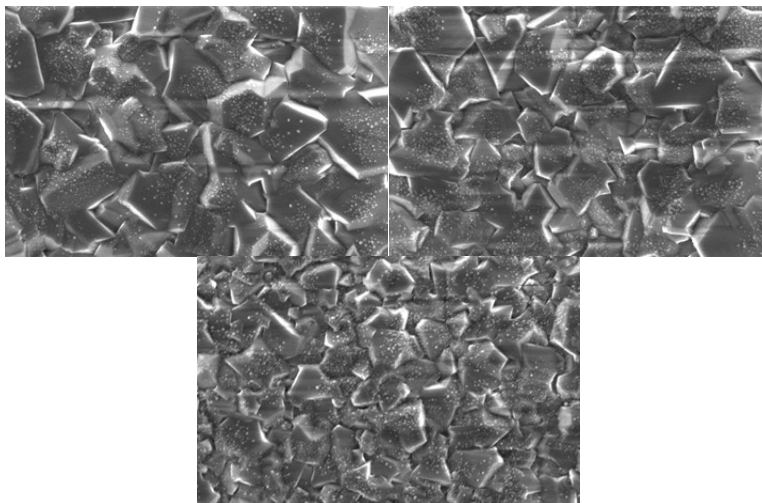


Figure 3.10 Typical SEM images of diamond films deposited (a) without excimer laser irradiation on the flame, and with excimer laser irradiation at frequencies of (b) 1, (c) 5, (d) 10, (e) 15, (f) 20, (g) 25, (h) 30 and (i) 35 Hz, respectively.

Diamond films were grown for 30 min on the WC substrates with different the excimer laser frequencies ranging from 1 to 35 Hz and fixed fluence of 170 mJ/cm^2 . Fig. 3.10 shows the SEM images of the morphologies of the diamond films. Fig. 3.10 shows that the average size of the diamond crystals decreased with the frequency of the excimer laser increased. It is also observed that the size of the diamond grains deposited with excimer laser irradiation on the combustion flame became bigger than those deposited without excimer laser irradiation. It could be explained by that the species proportions during the deposition process were affected by excimer laser irradiation on the combustion flame with different frequencies. With eximer laser irradiation on the flame, carbon atoms in the flame were electronically excited. It enhanced chemical reactions on the diamond surface, so the formation of sp^3 bonding to diamond surface was easier. The number of secondary nucleation sites, which existed in the combustion flame CVD process, was decreased by the excited carbon atoms. However, with the excimer laser

frequency increasing, the reduction of the number of secondary nucleation sites decreased so the secondary nucleation site density increased, which resulted in a decrease of the average size of diamond grains.

Thickness of the diamond films deposited with different excimer laser frequencies irradiation on the WC substrates were measured by a stylus profiler as shown in Fig. 3.11 (a). Fig. 3.11 (b) shows the relationship between the thickness of the diamond films and the frequency of the excimer laser. Diamond film thickness increased from 9 to 20 μm approximately as the excimer laser frequency increased from 1 to 35 Hz. With excimer laser irradiation on the combustion flame, the deposited diamond films were thicker than that without excimer laser irradiation. The deposition rate of diamond film increased with the excimer laser frequency increasing. With eximer laser irradiation on the flame, chemical reactions were enhanced on the diamond surface by electronically excited carbon atoms. It was easier to the form sp^3 bonding to diamond surface. Therefore, diamond film deposition rate was promoted.

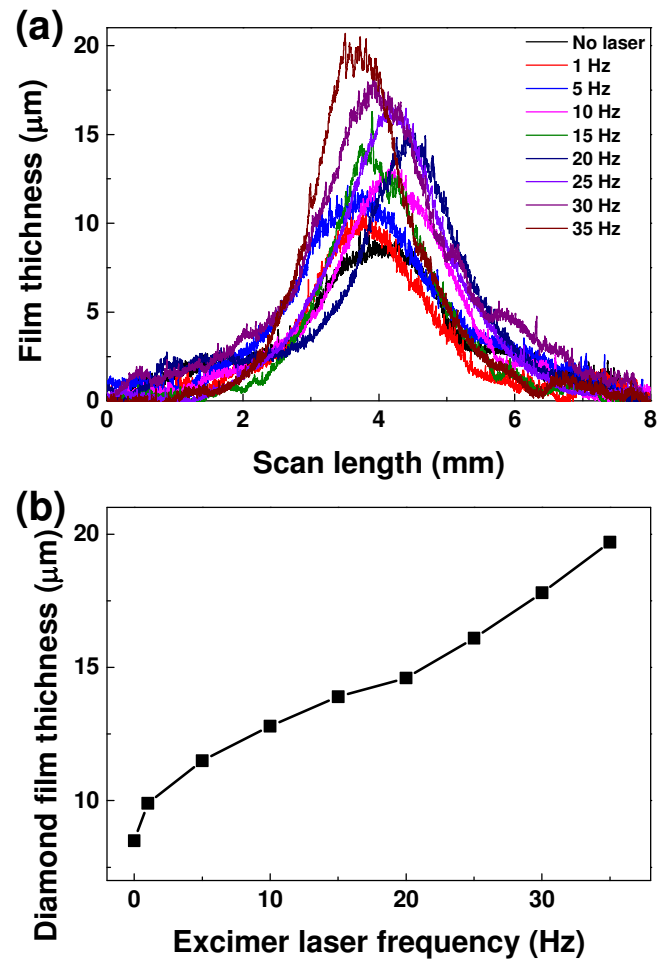


Figure 3.11 (a) Thickness of diamond films deposited with excimer laser irradiation at different laser frequencies on the flame and (b) the relationship between laser frequency and film thickness.

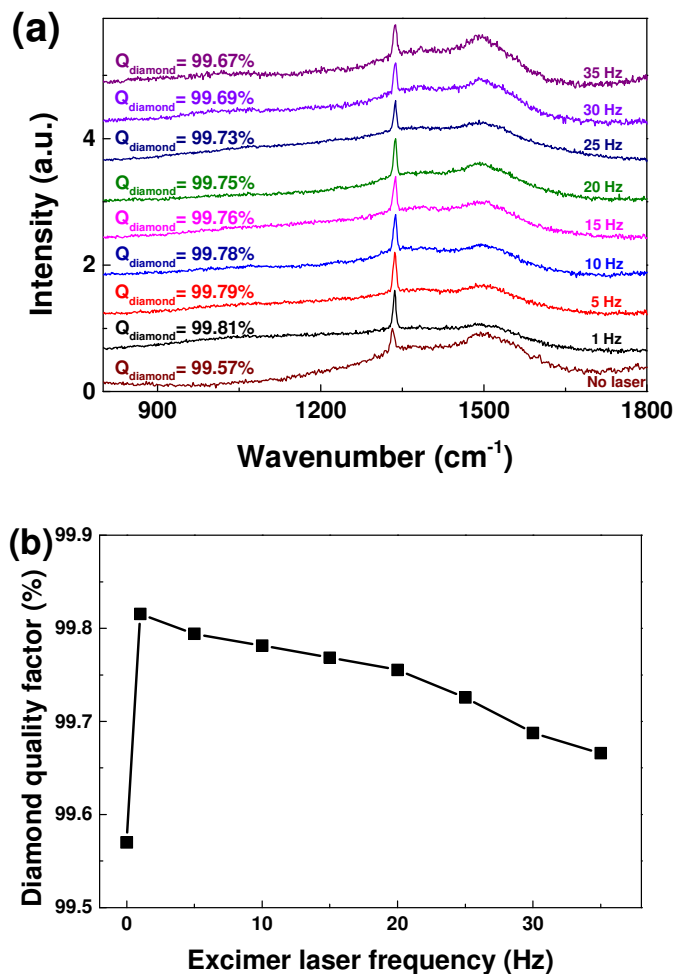


Figure 3.12 (a) Typical Raman spectra of diamond films deposited with excimer laser irradiation at different laser frequencies on the flame and (b) the relationship between laser frequency and diamond quality factor.

Fig. 3.12 (a) shows the Raman spectra of the diamond films deposited with different excimer laser frequency irradiation on the diamond films. Sharp diamond peaks are observed at around 1332 cm^{-1} . G-bands around 1500 cm^{-1} stand for amorphous carbon. It is obvious that the G-bands were changing with the excimer laser frequency increasing.

The diamond quality was evaluated by the diamond quality factor, which was calculated by the function

$$Q_{diamond} = \frac{I_{diamond\ peak}}{I_{diamond\ peak} + \frac{I_{carbon-bonds}}{233}} \times 100\% [20].$$

As shown in Fig. 3.12 (b), with the frequency of the excimer laser increased from 1 to 35 Hz, the quality of the diamond films decreased. Compared to that without excimer laser irradiation, higher-quality diamond films were deposited with excimer laser irradiation on the flame.

As high-energy surface, grain boundaries constituted preferential locations for impurities incorporation. Therefore, this imperfection of diamond was much easier to deposit non-diamond carbon. With excimer laser frequency increasing, the average size of diamond grains decreased, which induced a decrease of diamond film quality.

3.2.2.3 Absorption of the excimer laser by the combustion flame

The experimental setup was similar with what was shown in Fig. 3.6. A power meter was used to measure the power of the excimer laser before and after passing through the combustion flame. Then these two measured values were compared with each other to determine the laser absorption rate by the flame. The laser absorption rate was calculated by the function

$$Laser\ absorption\ rate = \frac{Laser\ power_{before} - Laser\ power_{after}}{Laser\ power_{before}}.$$

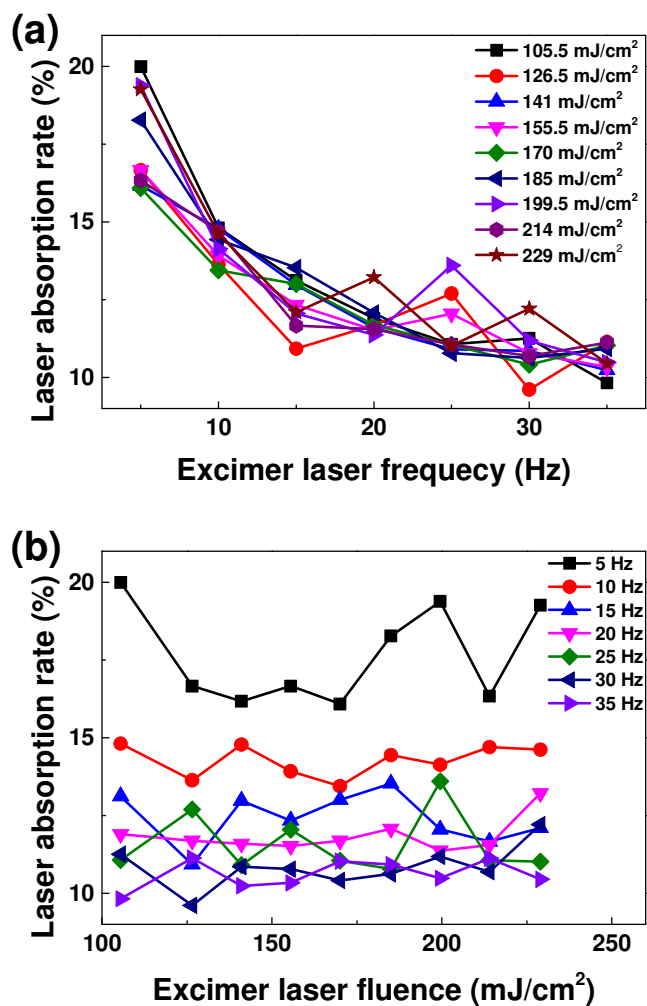


Figure 3.13 Absorption of excimer laser (a) at different frequencies from 1 to 35 Hz and (b) at different fluence from 105.5 to 229 mJ/cm^2 by $C_2H_4/C_2H_2/O_2$ combustion flame.

Fig. 3.13 shows the laser energy absorption rate of the $C_2H_4/C_2H_2/O_2$ combustion flame with excimer laser irradiation at different laser frequencies and different laser fluences. The relationship between laser absorption and excimer laser frequency is shown in Fig. 3.13 (a). It is observed that at all the fluence of the excimer laser, the absorption rate of the excimer laser by the combustion flame decreased with the frequency increasing. The energy absorbed by the flame decreased from the highest 20% to the

lowest 10% of the incident excimer laser energy. Fig. 3.13 (b) exhibits that the relationship between the absorption rate of the excimer laser with the excimer laser fluence. The absorption of the excimer laser with different laser fluences was steady. According to Fig. 3.13, it is believed that energy coupled into the flame via electron excitation of carbon atoms by excimer laser irradiation on the flame occurred during diamond film deposition.

Excimer laser irradiation on the flame can electronically excite carbon atoms in the flame, which enhanced the chemical reactions on the diamond film surface. It decreased secondary nucleation sites produced by the combustion flame. With a higher excimer laser frequency irradiation on the flame, the laser absorption rate by the combustion flame became smaller. The number of carbon atoms electronically excited by one excimer laser pulse decreased, leading to a decrease of the formation of sp^3 bonding to diamond surface. Thus, secondary nucleation sites produced by the flame increased. However, the energy coupled into the flame increased, which led to an increase of growth rate. Therefore, the average size of diamond grains decreased but the deposition rate increased. Due to the decrease of crystal size, grain boundaries increased and diamond quality decreased.

On the other hand, as the excimer laser fluence increased, the absorption rate was almost the same at a fixed laser frequency. The energy coupled into the flame increased and the number of excited carbon atoms increased. Therefore, the growth rate was enhanced and the secondary nucleation sites produced by the flame decreased. As a result, with increasing excimer laser fluence irradiation on the flame, the diamond grain sizes, deposition rate and the deposited diamond film quality increased.

3.2.3 *Post-growth excimer laser irradiation on diamond films*

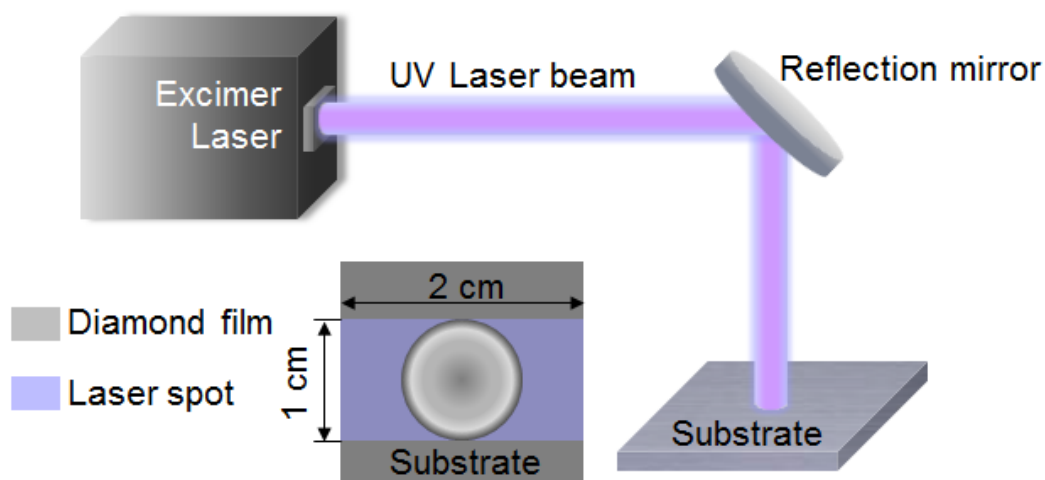


Figure 3.14 A schematic diagram showing the experimental setup for *post-growth* KrF excimer laser irradiation on diamond films.

As shown in Fig. 3.14, a schematic diagram of the experimental setup for *post-growth* excimer laser irradiation on diamond films. Diamond films have been deposited on the WC plates (BS-6S, Basic Carbide Corp., containing 6% cobalt). Low-quality diamond film with much non-diamond carbon content on the surface was chosen as the sample diamond film so that the changes on the surface of the diamond film were obvious to evaluate. The 248 nm KrF excimer laser was used to irradiate the sample. The excimer laser was introduced to the diamond film sample, which was perpendicular to the substrates. Due to the $1 \times 2 \text{ cm}^2$ laser beam spot size, the laser beam can cover the whole deposition area on the substrate with a diameter of around 9 mm. In this experiment, the fluence of the excimer laser was fixed at 234 mJ/cm^2 . And the excimer laser frequency was set to 1 Hz. With increasing the number of the excimer laser irradiation pulses, the

sample diamond film irradiated by the excimer laser were characterized to investigate the effect of *post-growth* excimer laser irradiation.

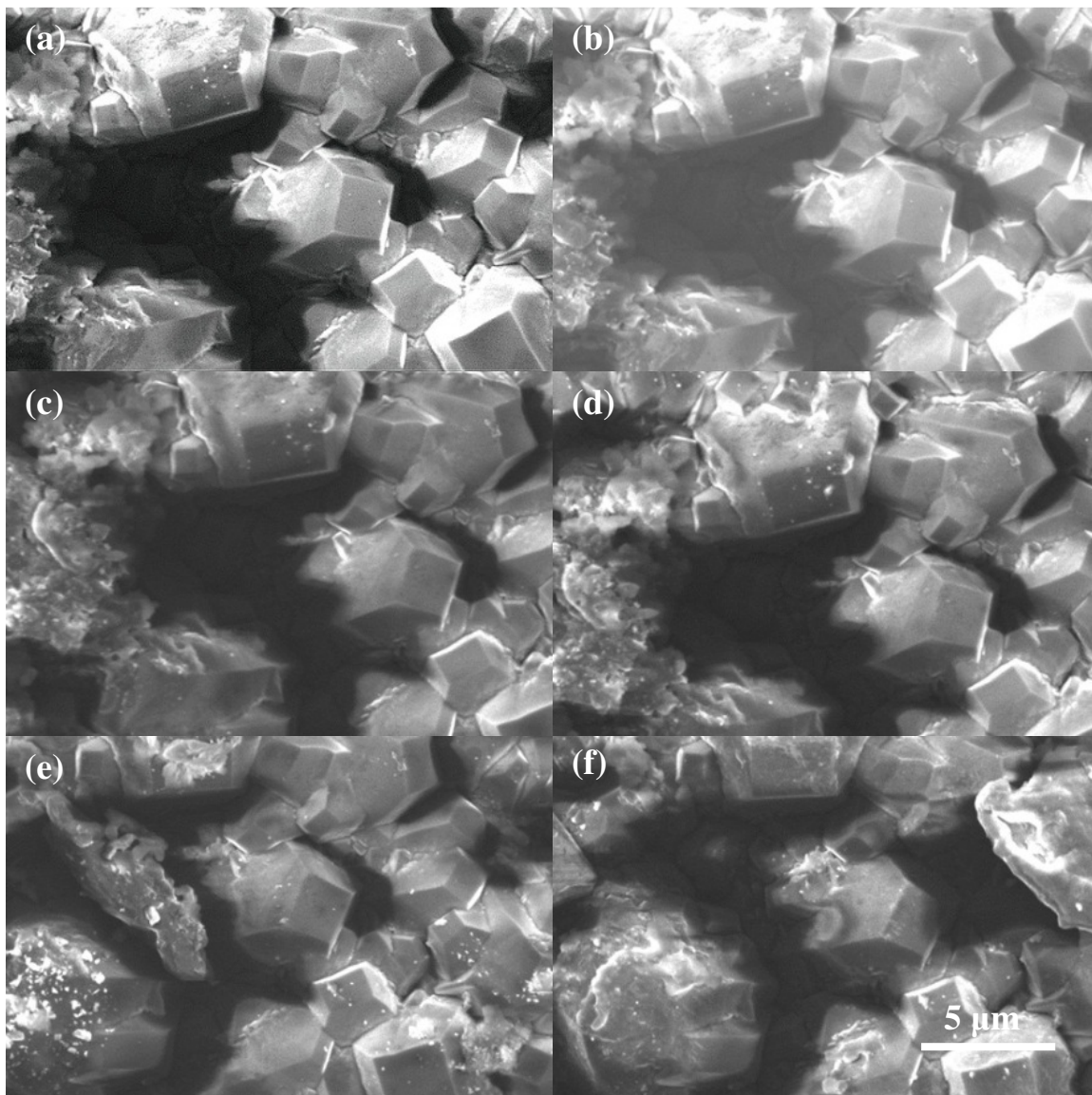


Figure 3.15 Typical SEM images of a diamond film (a) not irradiated by excimer laser, irradiated by excimer laser with (b) 10, (c) 20, (d) 30, (e) 40 and (f) 50 pulses, respectively.

As Fig. 3.15 shown, the morphologies of the same position on the diamond film irradiated by excimer laser with different pulses were characterized by the SEM images. Fig. 3.15 (a) shows the original morphology of the sample as the control group. Fig. 3.15 (b)-(f) show that the same sample was irradiated by the excimer laser with 10 to 50 pulses, respectively. Compared with the original diamond film sample, the area of non-diamond carbon (black part) between the diamond grains was smaller with 10-pulse excimer laser irradiation, as shown in Fig. 3.15 (b). It is obvious that the non-diamond carbon area decreased in Fig. 3.15 (c) and (d), due to non-diamond carbon removal. It is also noticed that parts of diamond grains were damaged and that new non-diamond carbon content was produced in Fig. 3.15 (e) and (f). The diamond crystal lattice was also broken with the white spot generation regarded as defects.

When the number of the excimer laser pulses was less than around 30, non-diamond carbon was removed by excimer laser irradiation and few defects were produced. However, when the number of the excimer laser pluses was more than 30, non-diamond carbon content was produced by the oxidation or graphitization of the diamond film surface. In addition, the number of white spots increased with increasing excimer laser pulses, indicating more defects generated on the surface shown in Fig. 3.15 (e) and (f). Therefore, it was verified that the explanation of the excimer laser irradiation on the diamond film influencing the seeding and nucleation process during diamond film deposition as we discussed in session 3.2.1.

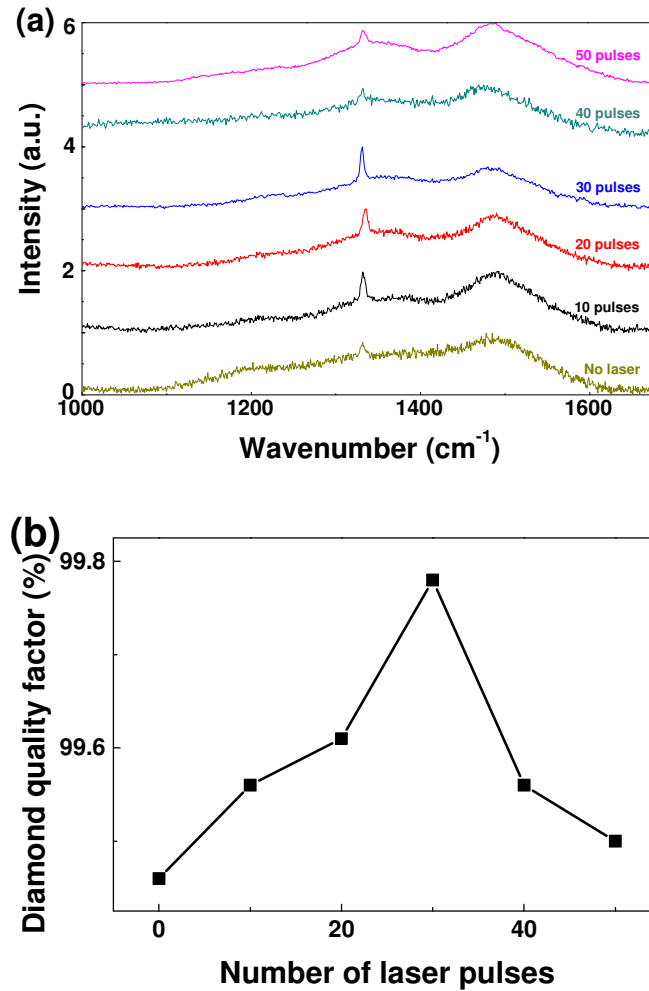


Figure 3.16 (a) Typical Raman spectra of the sample diamond film not irradiated by excimer laser, irradiated by excimer laser with 10, 20, 30, 40 and 50 pulses and (b) the relationship between the number of laser pulses and diamond quality factor.

The quality of diamond films was characterized by a Raman system. Fig. 3.16 (a) shows the Raman spectra of the sample diamond films irradiated by excimer laser with 10 to 50 pulses and the Raman spectra of the original diamond film. Diamond peaks are observed at around 1332 cm⁻¹. G-bands around 1500 cm⁻¹ appear in the spectra, standing for non-diamond carbon. When the pulse number of excimer laser increased from 0 to 30,

the intensity of diamond peak increased and the intensity of G-band decreased relatively. When the pulse number of excimer laser increased from 30 to 50, the intensity of diamond peak decreased and the intensity of G-band increased relatively. The diamond quality was evaluated by the diamond quality factor, which was calculated by the function of

$$Q_{diamond} = \frac{I_{diamond\ peak}}{I_{diamond\ peak} + \frac{I_{carbon-bonds}}{233}} \times 100\% [20].$$

Fig. 3.16 (b) illustrated that the quality of the sample diamond film was influenced by excimer laser irradiation. In a certain range of the pulse number, excimer laser can realize non-diamond carbon removal to improve the quality of diamond films. If the pulse number exceeded the range, oxidation or graphitization of diamond film surface can result in a decrease of the diamond film quality. It matched the phenomenon observed in Fig. 3.15.

3.3 Conclusions

The *in-situ* excimer laser irradiation during diamond film deposition was investigated. Two different *in-situ* excimer laser irradiation ways were studied in this chapter.

With excimer laser irradiation on the diamond film, the diamond film quality and thickness increased at relatively low laser fluence and decreased at relatively high fluence. However, the SEM images show the average size of the diamond grains decreased with the excimer laser fluence increasing. This phenomenon illustrated that the seeding and nucleation process during diamond deposition can be influenced by KrF excimer laser irradiation on the diamond film, due to the effect on non-diamond carbon removal, secondary nucleation sites generation and graphitization of diamond film surface.

With excimer laser irradiation on the combustion flame, the diamond film deposition rate increased. With the fluence increasing, the size of the diamond grains and the diamond film thickness and quality increased. However, with the excimer laser frequency increasing, the diamond crystal sizes and the diamond quality decreased. By measuring the absorption of excimer laser by flame, it is believed that KrF excimer laser irradiation via electron excitation of carbon atoms in combustion flame influenced diamond film deposition process.

Non-diamond carbon removal can be realized by *post-growth* excimer laser irradiation on diamond films. Within a safe range of excimer laser pulse number, the quality of diamond film can be improved by *post-growth* excimer laser irradiation. In addition, with relatively large number of laser pulses, defects of diamond grains and new non-diamond carbon content produced by *post-growth* excimer laser irradiation are

observed. This phenomenon verified that *in-situ* KrF excimer laser irradiation on the diamond film can influence the seeding and nucleation during diamond film deposition through the effect of non-diamond carbon removal, secondary nucleation sites generation and graphitization of diamond film surface.

This study shows that *in-situ* KrF excimer laser irradiation during combustion flame CVD of diamond films can be used to improve the deposition rate and the quality of the diamond films. On the other hand, *post-growth* excimer laser irradiation on diamond film can be regarded as a non-diamond carbon removal method.

References

- [1] J. Asmussen and D. K. Reinhard, *Diamond films handbook*, 1st ed. (CRC Press, 2002).
- [2] Hirose, H. and Komaki, K. Eur. Pat. Appl. EP324538 (1988).
- [3] J. B. Donnet, H. Oulanti, T. Le Huu, and M. Schmitt, "Synthesis of large single crystal diamond using combustion-flame method", *Carbon* **44**, 374 (2006).
- [4] Ling, H., Xie, Z. Q., Gao, Y., Gebre, T., Shen, X. K., and Lu, Y. F., "Enhanced chemical vapor deposition of diamond by wavelength-matched vibrational excitations of ethylene molecules using tunable CO₂ laser irradiation", *Journal of Applied Physics* **105**, 064901 (2009).
- [5] Ling, H., Sun, J., Han, Y. X., Gebre, T., Xie, Z. Q., and Zhao, M., "Laser-induced resonant excitation of ethylene molecules in C₂H₄/C₂H₂/O₂ reactions to enhance diamond deposition", *Journal of Applied Physics* **105**, 014901 (2009).
- [6] S. Marinkovic, S. Stankovic, and Z. Rakocevic, "Effects of cemented carbide surface pretreatment in combustion flame chemical vapour deposition of diamond", *Thin Solid Films* **354**, 118 (1999).
- [7] D. B. Oakes, J. E. Butler, K. A. Snail, W. A. Carrington, and L. M. Hanssen, "Diamond synthesis in oxygen-acetylene flames: Inhomogeneities and the effects of hydrogen addition", *Journal of Applied Physics* **69**, 2602 (1991).
- [8] K. A. Snail, R. G. Vardiman, J. P. Estrera, J. W. Glesener, C. Merzbacher, C. J. Craigie, C. M. Marks, R. Glosser, and J. A. Freitas, "Diamond growth in turbulent oxygen-acetylene flames", *Journal of Applied Physics* **74**, 7561 (1993).

- [9] T. J. Li, Q. H. Lou, J. X. Dong, Y. R. Wei, J. Zhou, J. R. Liu, Z. M. Zhang, and F. H. Sun, *Applied Surface Science* **193**, 102 (2002).
- [10] E. Cappelli, S. Orlando, F. Pinzari, A. Napoli, and S. Kaciulis, “WC - Co cutting tool surface modifications induced by pulsed laser treatment”, *Applied Surface Science* **139**, 376 (1999).
- [11] D. G. Lee, D. R. Gilbert, S. M. Lee, and R. K. Singh, “Surface composites: a novel method to fabricate adherent interfaces in thermal-mismatched systems”, *Composites Part B Engineering* **30**, 667 (1999).
- [12] F. H. Sun, M. Chen, Z. M. Zhang, and H. S. Shen, *Key Engineering Materials* **202-2**, 159 (2001).
- [13] H. G. Xue, F. H. Sun, Y. P. Ma, and M. Chen, “Deposition of Smooth Diamond Films with High Adhesive Strength on WC-Co Inserts and Their Cutting Performance in Turning GFRP”, *Key Engineering Materials* **329**, 755 (2007).
- [14] J. Narayan, V. P. Godbole, and C. W. White, “Laser Method for Synthesis and Processing of Continuous Diamond Films on Nondiamond Substrates”, *Science* **252**, 416 (1991).
- [15] T. P. Ong, F. L. Xiong, R. P. H. Chang, and C. W. White, “Mechanism for diamond nucleation and growth on single crystal copper surfaces implanted with carbon”, *Applied Physics Letters* **60**, 2083 (1992).
- [16] S. J. Lin, S. L. Lee, J. Hwang, C. S. Chang, and H. Y. Wen, “Effects of local facet and lattice damage on nucleation of diamond grown by microwave plasma chemical vapor deposition”, *Applied Physics Letters* **60**, 1559 (1992).

- [17] S. J. Lin, S. L. Lee, J. Hwang, and T. S. Lin, "Selective Deposition of Diamond Films on Ion-Implanted Si(100) by Microwave Plasma Chemical Vapor Deposition", *Journal of the Electrochemical Society* **139**, 3255 (1992).
- [18] J. B. Donnet, D. Paulmier, H. Oulanti, and T. Le Huu, "Diffusion of cobalt in diamond films synthesized by combustion flame method", *Carbon* **42**, 2215 (2004).
- [19] M. Alam, D. E. Peebles, and D. R. Tallant, "Diamond deposition onto WC-6%Co cutting tool material: coating structure and interfacial bond strength", *Thin Solid Films* **300**, 164 (1997).
- [20] Stephanie R. Sails, Derek J. Gardiner, Michael Bowden, James Savage and Don Rodway, "Monitoring the quality of diamond films using Raman spectra excited at 514.5 nm and 633 nm", *Diamond and Related Materials*, Volume **5**, 589 (1996).
- [21] V. N. Strekalov, V. I. Konov, V. V. Kononenko, and S. M. Pimenov, "Early stages of laser graphitization of diamond", *Applied Physics A Materials Science & Processing* **76**, 603 (2003).

CHAPTER 4

Multi-torch Diamond Film Deposition

4.1 Introduction

4.2 Experiments, results and discussion

4.3 Conclusions

4.1 Introduction

In 1988, Hirose and Komaki invented a CVD method to deposit diamond films on non-diamond substrates by using combustion flame in the open air [1]. Because it is the only way to grow diamond thin films in the open air, this method opened a new area for diamond film deposition. Up to now, the fast growth rate for combustion CVD of diamond films can reach to 60 $\mu\text{m/hr}$ approximately [2]. Additionally, large individual crystal has been achieved by using combustion flame CVD [3,4]. However, not only large crystal diamond, but also larger-area diamond thin film can be used for industrial applications. As a functional coating, diamond thin film can be used for wear resistance, surface protection, thermal management, optical windows, acoustic speakers, active electronic devices, sensors and photon and electron emitters [5-13]. Because of these attractive applications, large-area diamond thin films have been synthesized successfully by MPCVD [14].

As the most flexible CVD, combustion flame CVD of diamond films has advantages of scalable nature, minimal utility requirements, high growth rate and significantly reduced capital cost [14]. Nevertheless, due to the limitation of the torch size, the size of the combustion flame CVD diamond film is relatively small compared to other CVD methods. In order to address this challenge, we applied multi-torch method to enlarge the area of diamond thin films. Considering that it took a long time to deposit large continuous diamond thin films with one torch, the multi-torch method can highly shorten the time with a high efficiency of diamond thin films deposition. In order to grow high-quality diamond with high growth rate, we introduced CO_2 laser into the $\text{C}_2\text{H}_4/\text{C}_2\text{H}_2/\text{O}_2$ combustion flame with resonant vibrational excitation of ethylene [15,16].

4.2 Experiments, results and discussion

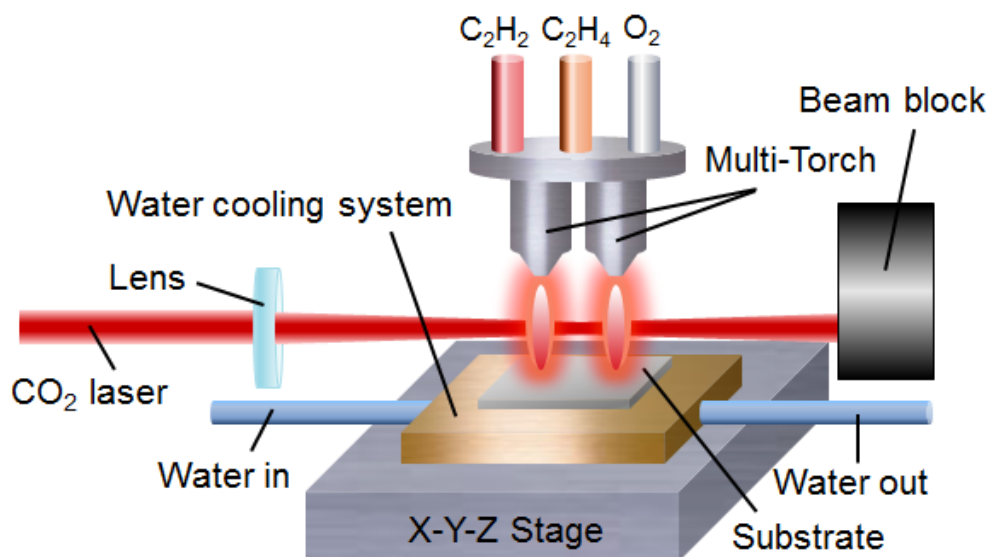


Figure 4.1 A schematic diagram of the experimental setup for large continuous diamond thin films deposition using combustion flame CVD with CO₂ laser excitation.

The experimental setup is shown in Fig. 4.1. A multi-torch setup was applied which was a combination of two same torches. The diameter of the orifice was 1.5 mm. Two torches were used to generate two C₂H₄/C₂H₂/O₂ combustion flames separately. The distance between the two torches was 1 cm. C₂H₄, C₂H₂ and O₂ were mixed up with a volume ratio of 1:0.87:1.93. This flow rates were controlled by six mass flow controllers (B7920V, Spec-Air Gases & Technologies). The WC substrates (BS-6S, Basic Carbide Corp., containing 6% cobalt) with dimensions of 39.2 × 39.2 × 1.6 mm³ were placed on the water cooling system which was fixed on an X-Y-Z stage with motors. A wavelength-tunable CO₂ laser (PRC, spectrum range from 9.2 to 10.9 μm) was to assist the combustion flame diamond film deposition with resonant vibrational excitation of C₂H₄

precursor molecules. Laser energy was couple into the combustion flame by resonant vibrational excitation. The CO₂ laser was fixed to 10.532 μm with a power of 800 W and was introduced in parallel to the substrate but normal to the combustion flame axis. The laser was focused to a spot with 2 mm diameter by using a ZnSe convex lens of 254 mm focal length which matched the size of the inner flame. The length of the two inner flames was around 6 mm, but they shrunk to around 4 mm after the CO₂ laser went through the combustion flame, as Fig. 4.2 shown. The gap distance was fixed at 0.5 mm. The temperature of the substrate surface was monitored by pyrometer (Omega Engineering, Inc., OS3752) and it was controlled at 760 to 780 °C by controlling the water flow in the cooling system. To grow larger-area diamond thin films, the multi-torch setup needed to move slowly through the whole deposition area with step by step. Each step was 2.5 mm. In this chapter, we controlled the deposition time per step (time/step) to grow diamond thin films with an area of 2.5 × 2.5 cm² on WC substrates. Fig. 4.3 shows the scanning path of the multi-torch to grow larger-area diamond films.

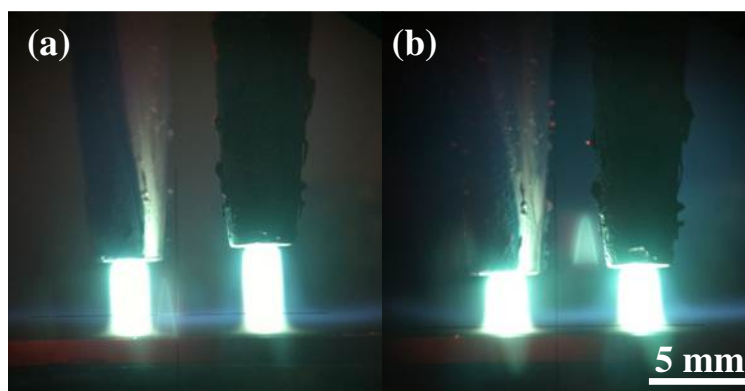


Figure 4.2 Images of multi-torch flames (a) without laser, (b) with CO₂ laser resonant vibrational excitation at 10.532 μm, 800 W.

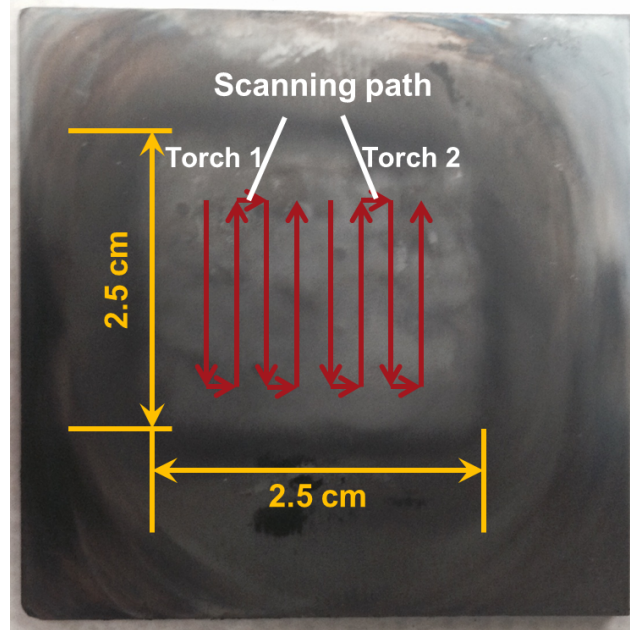


Figure 4.3 An optical image of diamond thin film.

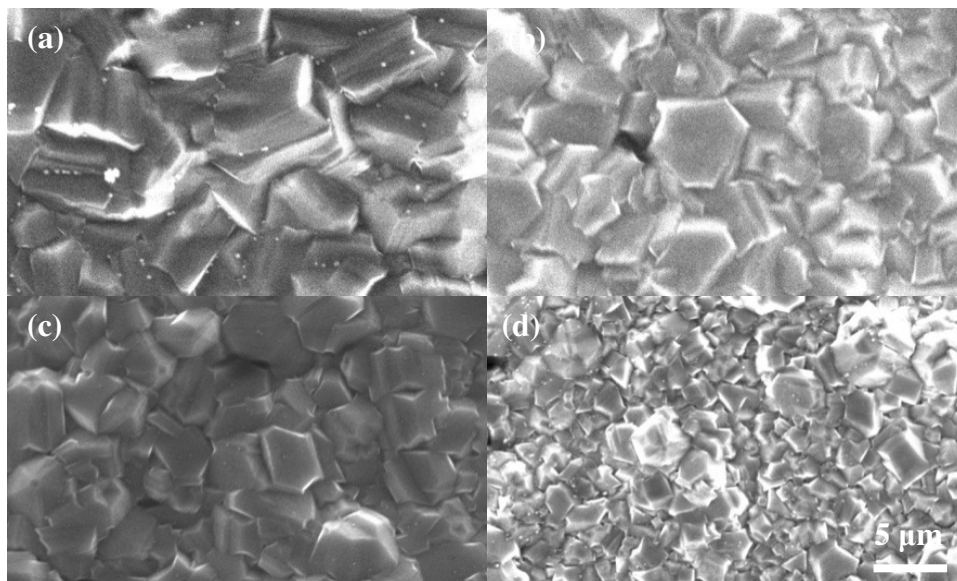


Figure 4.4 Typical SEM images of diamond thin films deposited with 10.532 μm CO₂ laser excitation at different deposition time per step of (a) 15, (b) 10 and (c) 5 min and (d) without CO₂ laser excitation at a deposition time per step of 10 min, respectively.

Fig. 4.4 (a)-(c) shows that the SEM images of the diamond films with CO₂ laser excitation to the combustion flame at three different time/step, 15, 10 and 5 min. It is observed that the average size of the diamond grains decreased with the time/step decreasing, due to the decrease of deposition time. Compared with Fig. 4.4 (d), it is believed that the diamond crystals deposited with CO₂ laser excitation had better uniformity and larger size than those without CO₂ laser excitation. This can be explained by that the CO₂ laser excitation to the combustion flame significantly influenced the deposition process including deposition temperature and species proportion [6, 7].

Thickness of the diamond films deposited with CO₂ laser excitation by using the multi-torch at different time/step and deposited without CO₂ laser excitation was measured by a stylus profiler as shown in Fig. 4.5. Diamond film thickness increased from 6 μm to 16 μm as the time/step increased from 5 min to 15 min. With CO₂ laser excitation, the deposited diamond film was thicker than that without CO₂ laser excitation. The reason why the deposition rate of the diamond films increased was that the deposition time increased.

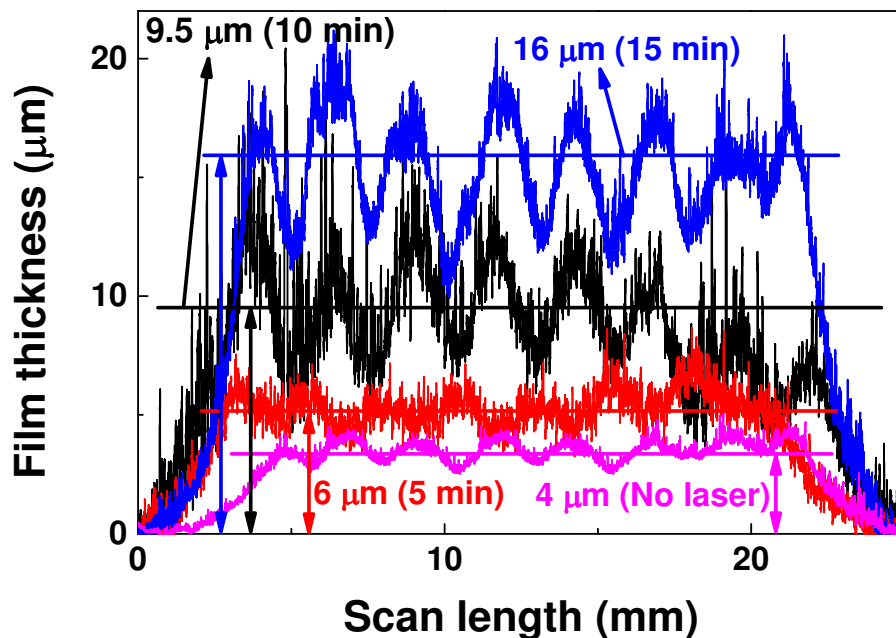


Figure 4.5 Thickness of diamond films deposited with 10.532 μm CO_2 laser excitation at different deposition time per step of 15, 10 and 5 min and without CO_2 laser excitation at a deposition time per step of 10 min.

The diamond film quality was characterized by a Raman system. Raman spectra of the diamond films deposited with CO_2 laser excitation at different time/step and without CO_2 laser excitation are shown in Fig. 4.6. Sharp diamond peaks are observed at around 1332 cm^{-1} . G-bands around 1500 cm^{-1} appeared in the spectra. With higher time/step, the higher-quality diamond films can be deposited. It is believed that diamond thin films with higher quality can be deposited with longer deposition time. Without CO_2 laser excitation, the Raman spectroscopy shows a weaker peak at 1332 cm^{-1} and a stronger G-band than that with CO_2 laser excitation. It indicates that high-quality diamond films were grown with CO_2 laser resonant vibrational excitation.

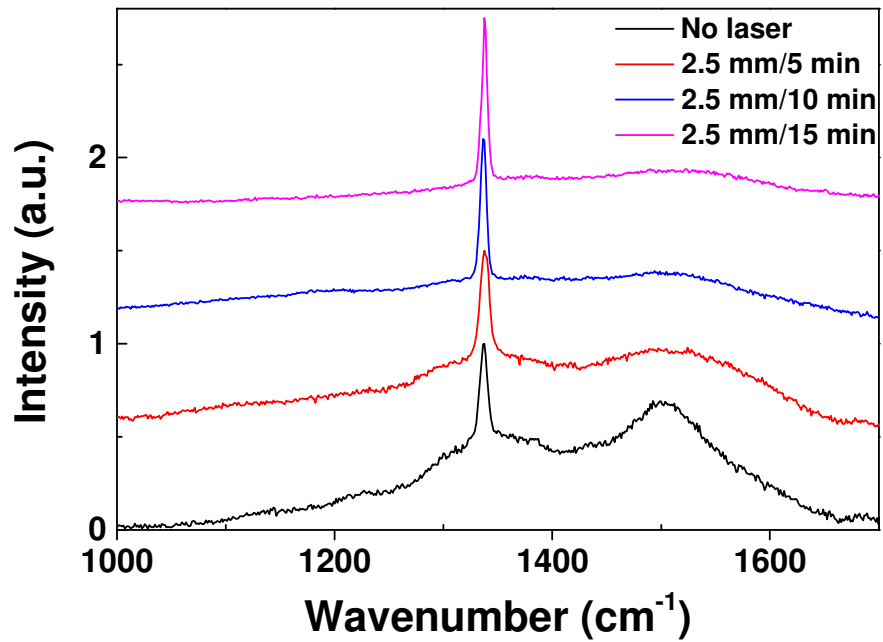


Figure 4.6 Raman spectra of diamond films deposited with 10.532 μm CO₂ laser excitation at different deposition time per step of 15, 10 and 5 min and without CO₂ laser excitation at a deposition time per step of 10 min.

4.3 Conclusions

A laser-assisted multi-torch deposition was developed for growing large-area diamond thin films by resonant vibrational excitation of ethylene molecules. The $2.5 \times 2.5 \text{ cm}^2$ diamond thin films were obtained. The resonant vibrational excitation enhanced the combustion flame to grow diamond films with high deposition rate and high quality. With increasing the deposition time per step, the quality of diamond film increased. With maintaining high-quality diamond film deposition, multi-torch method can improve the efficiency of growing diamond thin films using combustion flame CVD.

References

- [1] Hirose, H. and Komaki, K. Eur. Pat. Appl. EP324538 (1988).
- [2] Alers, P., Hanni, W., and Hintermann, H. E., "A comparative study of laminar and turbulent oxygen-acetylene flames for diamond deposition", *Diamond and Related Materials* **2**, 393 (1992).
- [3] Abe, T., Suemitsu, M., Miyamoto, N., and Sato, N., "Formation of 250- μm -diameter diamond crystals by combustion flame method: Effects of preformation of molybdenum oxide on the substrate", *Journal of Applied Physics* **73**, 971 (1993).
- [4] Wang, X. H., Zhu, W., Vonwindheim, J., and Glass, J. T., "Combustion growth of large diamond crystals", *Journal of Crystal Growth* **129**, 45 (1993).
- [5] V.G. Ralchenko, A.A. Smolin, V.I. Konov, K.F. Sergeichev, I.A. Sychov, I.I. Vlasov, V.V. Migulin, S.V. Voronina, A.V. Khomich, "Large-area diamond deposition by microwave plasma", *Diamond and Related Materials* **6**, 417 (1997).
- [6] V. Shanov, W. Tabakoff, and R. N. Singh, "CVD diamond coating for erosion protection at elevated temperatures", *Journal of Materials Engineering and Performance* **11**, 220 (2002).
- [7] C. A. Klein, "Diamond windows for IR applications in adverse environments", *Diamond and Related Materials* **2**, 1024 (1993).
- [8] W. D. Brown, R. A. Beera, H. A. Naseem, and A. P. Malshe, "State-of-the-art synthesis and post-deposition processing of large area CVD diamond substrates for thermal management", *Surface & Coatings Technology* **86-87**, 698 (1996).

- [9] F. Deuerler, O. Lemmer, M. Frank, M. Pohl, and C. Hessian, “Diamond films for wear protection of hardmetal tools”, *International Journal of Refractory Metals & Hard Materials* **20**, 115 (2002).
- [10] P. H. Cutler, N. M. Miskovsky, P. B. Lerner, and M. S. Chung, *Applied Surface Science* **146**, 126 (1999).
- [11] P. R. Chalker and C. Johnston, “The use of internal field emission to inject electronic charge carriers into the conduction band of diamond films: a review”, *Physica Status Solidi A-Applied Research* **154**, 455 (1996).
- [12] M. D. Whitfield, B. Audic, C. M. Flannery, L. P. Kehoe, G. M. Cream, C. Johnston, P. R. Chalker, and R. B. Jackman, “Polycrystalline diamond films for acoustic wave devices”, *Diamond and Related Materials* **7**, 533 (1998).
- [13] E. Wu, V. Jacques, F. Treussart, H. Zeng, P. Grangier, and J. F. Roch, “Single-photon emission in the near infrared from diamond colour centre”, *Journal of Luminescence* **119**, 19 (2006).
- [14] K. Okano, K. Hoshina, M. Iida, S. Koizumi, and T. Inuzuka, “Fabrication of a diamond field emitter array”, *Applied Physics Letters* **64**, 2742 (1994).
- [15] Ling, H., Xie, Z. Q., Gao, Y., Gebre, T., Shen, X. K., and Lu, Y. F., “Enhanced chemical vapor deposition of diamond by wavelength-matched vibrational excitations of ethylene molecules using tunable CO₂ laser irradiation”, *Journal of Applied Physics* **105**, 064901 (2009).

- [16] Ling, H., Sun, J., Han, Y. X., Gebre, T., Xie, Z. Q., and Zhao, M., “Laser-induced resonant excitation of ethylene molecules in C₂H₄/C₂H₂/O₂ reactions to enhance diamond deposition”, *Journal of Applied Physics***105**, 014901 (2009).

CHAPTER 5

Summary of Current Work and Suggested Future Directions

5.1 Summary of current work

5.2 Suggested future directions

5.1 Summary of current work

In this study, efforts were made to explore the capability of a laser-assisted combustion flame CVD technique, in which a KrF excimer laser irradiation was used for improving diamond thin film quality and deposition rate. Applying KrF excimer laser is aiming to: 1) achieve energy coupling into combustion flame; 2) influence species proportions in the combustion flame; 3) promote seeding and nucleation process during diamond film deposition; 4) increase the diamond thin film quality and deposition rate through non-diamond carbon removal. The research efforts mainly focus on following activities, including: 1) studying the influence of the gap distance between the inner flame and the substrates on crystallographic orientations of diamond films, diamond film quality and deposition rate to determine the optimal parameters for diamond film deposition; 2) conducting *in-situ* KrF excimer laser irradiation during diamond thin film deposition to increase the quality and the growth rate of diamond thin film with the optimal deposition parameters, which includes excimer laser irradiation on diamond films and on the combustion flame; 3) applying *post-growth* KrF excimer laser irradiation on diamond films, which is aiming to understand and verify the effect of *in-situ* KrF excimer laser irradiation on diamond thin films during the deposition. A highly efficient method with multi-torch is also developed for synthesizing large-area diamond films.

Via using the combustion flame CVD method to grow diamond films, different gap distance between the inner flame and the substrate was studied to modify diamond surface morphology. As the gap distance increasing, diamond film quality increased, but diamond deposition rate decreased. When the gap distance was fixed smaller than 0.3 mm, {1 0 0}-oriented diamond films can be deposited successfully. When the gap

distance was ~ 0.5 mm, $\{1\ 1\ 1\}$ -oriented diamond films with relatively high quality and relatively large thickness can be obtained. Moreover, little diamond film can be deposited with gap distance larger than 0.8 mm. On the other hand, this series of experiments were also regarded as a preparing part for all the experiments in this thesis, aiming to find the best gap distance in combustion flame CVD through investigating the influence of the gap distance to diamond thin film deposited.

Excimer laser irradiation on the diamond film was applied during combustion flame CVD of diamond films. Diamond films deposited with excimer laser irradiation on the diamond films have relatively larger crystal size, better quality and faster deposition rate, compared to those synthesized without excimer laser irradiation. The quality and deposition rate of diamond films increased as the laser fluence increasing from 52.8 to 70.5 mJ/cm^2 and decreased as the laser fluence increasing from 70.5 to 85 mJ/cm^2 . However, the average size of the diamond grains decreased with the excimer laser fluence increasing. This study indicates that *in-situ* KrF excimer laser irradiation on the diamond film can affect the seeding and nucleation process.

In-situ excimer laser irradiation on combustion flame was addressed to deposit diamond films. Different from the *in-situ* excimer laser irradiation on diamond films, the excimer laser was introduced to the flame parallel to the substrate. Compared with the diamond films deposited without excimer laser irradiation, those with *in-situ* excimer laser irradiation on the combustion flame had larger crystal size, higher quality and faster deposition rate. With the increase of laser fluence, the quality and the deposition rate of diamond films as well as the average size of diamond grains increased. With the increase of excimer laser frequency, the size of the diamond crystals and the diamond quality

decreased but the thickness of diamond films increased. Furthermore, through studying the absorption of excimer laser by flame, excimer laser energy was coupled into flame with electron excitation of carbon atoms in the flame.

Post-growth excimer laser irradiation on synthesized diamond films was developed as a laser-assisted non-diamond carbon removal method to improve the diamond film quality. By controlling excimer laser pulse number, non-diamond carbon can be efficiently removed by *post-growth* excimer laser irradiation within a certain number of laser pulses. As a result, the diamond film quality was much more improved. When the number of laser pulses increased larger, the diamond thin film surface was oxidation or graphitization and the defects were produced. Based on these results, it was verified that the *in-situ* KrF excimer laser irradiation on the diamond film can influence the seeding and nucleation process by non-diamond carbon removal, secondary nucleation sites generation and graphitization of diamond film surface.

To grow large-area diamond thin film, a multi-torch setup with CO₂ laser resonant excitation of C₂H₄ was developed. The large-area diamond film deposition process was accelerated due to applying multi-torch setup. With the increase of the deposition time/step of the multi-torch, the quality of diamond film and the deposition rate increased.

5.2 Suggested future directions

As the results shown in chapter 3 and the summary work in session 5.1, excimer laser irradiation on the flame enhanced diamond thin film deposition, including improving the diamond quality, increasing diamond deposition rate and enlarge the average size of diamond grains, via promoting diamond nucleation and changing the species proportions. Diamond film deposition process was significantly affected by proportions of radicals and the temperature. Different species in deposition process can influence the different properties of diamond films. Moreover, different species in deposition process can be excited by different wavelength laser. By controlling excited species in the deposition process, the mechanism can be studied in a very accurate way. Due to the thermal effect generated by continuous lasers, pulsed lasers can more efficiently active species from low energy states to high energy states through electron excitation. By controlling the energy coupling process via activation of the species in diamond deposition, diamond film deposition is controllable.

Fig. 5.1 shows the optical emission spectra of the combustion flame with a gas mixture of $C_2H_4/C_2H_2/O_2$. As shown in Fig. 5.1, many species are obtained in the spectra such as CH, C_2 OH and so on. As reported, CH and C_2 can enhance the secondary nucleation process to influence the size of diamond grains and deposition rate. OH can influence diamond film deposition with oxidation and etching of amorphous carbon and diamond grains. However, these explanations on the effect of radicals and the mechanism of diamond deposition are still unclear. By changing the wavelength of pulse lasers, species proportions in the diamond deposition process can be changed relatively.

Therefore, the changes in properties of the diamond film deposited by the combustion flame CVD can be studied by controlling the *in-situ* pulsed laser irradiation.

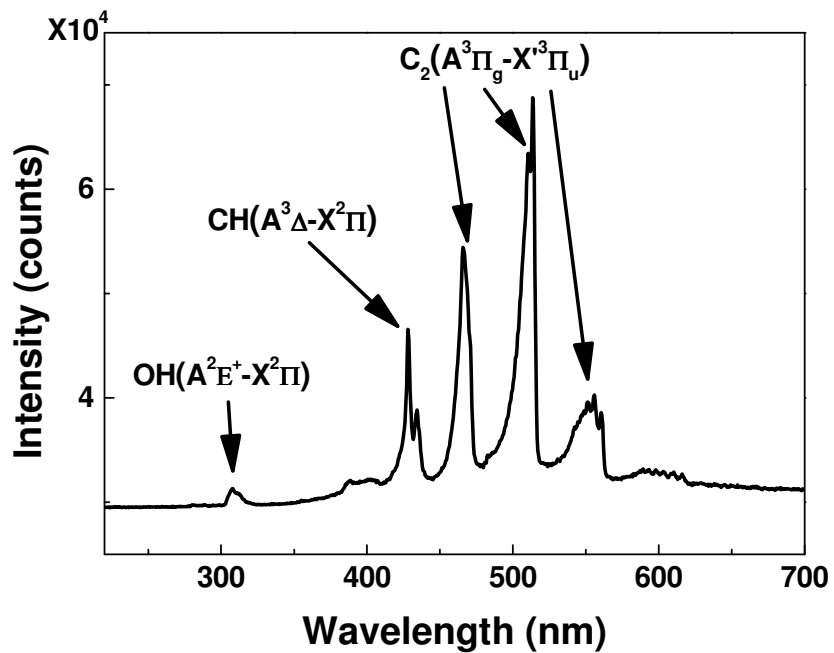


Figure 5.1 Optical emission spectra of $C_2H_4/C_2H_2/O_2$ combustion flame.

LIST OF PUBLICATIONS

Journal papers

1. L. S. Fan, Y. S. Zhou, **M. X. Wang**, Y. Gao, L. Liu, Y. F. Lu "Resonant vibrational excitation of ethylene molecules in laser-assisted diamond deposition" Laser Physics Letter (accepted).
2. L. Liu, S. Li, X. He, X. Huang, C. Zhang, L. Fan, **M. X. Wang**, Y. Zhou, K. Chen, L. Jiang, J. Silvain, and Y. Lu, "Flame-enhanced laser-induced breakdown spectroscopy," Opt. Express 22, 7686-7693 (2014).